$^{40}AR/^{39}AR$ AGES OF INTRUSIVE ROCKS FROM THE HENRY AND LA SAL MOUNTAINS, UTAH

by

Stephen T. Nelson
Matthew T. Heizler
Jon P. Davidson

OPEN-FILE REPORT 231 **DECEMBER 1991**
UTAH GEOLOGICAL SURVEY
a division of
UTAH DEPARTMENT OF NATURAL RESOURCES

$^{40}Ar/^{39}Ar$ AGES OF INTRUSIVE ROCKS FROM THE HENRY AND LA SAL MOUNTAINS, UTAH

Stephen T. Nelson, Department of Earth and Space Sciences, University of California, Los Angeles, Los Angeles, CA 90024-1567.

Matthew T. Heizler, Department of Earth and Space Sciences, University of California, Los Angeles, Los Angeles, CA 90024-1567.

Jon P. Davidson, Department of Earth and Space Sciences, University of California, Los Angeles, Los Angeles, CA 90024-1567.

ABSTRACT

Previously published Eocene and late-Oligocene K-Ar ages of intrusive rocks of the Henry and La Sal Mountains are bimodal whereas sphene and zircon fission-track ages are exclusively late-Oligocene. The apparent discordance between ages from the two techniques makes it difficult to understand the igneous activity in terms of regional geologic and tectono-magmatic events. Results of $^{40}Ar/^{39}Ar$ analyses reported here indicate that intrusive activity spanned several Ma during late-Oligocene time (23.3-31.2 Ma) and forms a time, as well as a spatial link between magmatism in the San Juan and Reno-Marysvale volcanic fields to the east and west respectively. Eocene K-Ar ages are shown to be the result of two discreet effects. First, excess argon is manifested in some samples by a trapped component of argon with a $^{40}Ar/^{36}Ar$ ratio that exceeds the atmospheric value (>295.5). We interpret other apparent Eocene K-Ar ages to result from heterogeneous excess argon, or inherited argon residing in incompletely outgassed hornblende xenocrysts in the rock.

Introduction

The Henry and La Sal Mountains intrusions are unique in terms of their laccolithic structure, magma compositions, and their setting within the Colorado Plateau. Understanding the age of igneous activity is critical to unraveling the origin of the intrusions and their regional tectono-magmatic context. Previous isotopic age determinations have been unable to resolve the age relationships of magmatism. K-Ar ages show a bimodal distribution of Eocene and Oligocene ages (Stern and others, 1965; Armstrong, 1969; and Dubiel and others, 1990), whereas fission-track ages are exclusively Oligocene to earliest Miocene (Sullivan, 1987; Sullivan and others, 1991). Cross-cutting relationships with the country rock can only constrain intrusive activity to post-Cretaceous (Hunt, 1953; 1958).

Geologic Setting

The intrusions occur in the Colorado Plateau interior (fig. 1), which is known to represent thick (50 km) cratonic crust (Thompson and Zoback, 1979; Allmendinger and others, 1987). Previous studies have shown that basement rocks in the region range from 1.6-1.9 Ga (Bennett and De Paolo, 1987; Karlstrom and others, 1987). The Colorado Plateau (fig. 1) is bounded by areas of intense Mesozoic and Cenozoic deformation and magmatism. The Laramide and Sevier belts, to the north, east, and west of the Colorado Plateau resulted from Cretaceous to Eocene crustal shortening. The mid-Tertiary "ignimbrite flare-up" produced voluminous magmatism of intermediate to silicic composition to the west (Reno-Marysvale belt), south (Mogollon-Datil belt) and east (San Juan field) that is contemporaneous with mid to late-Oligocene magmatism in the Henry and La Sal Mountains. Late-Cenozoic

(<17 Ma) basaltic magmatism has been largely restricted to the outer rim or structural transition zone between the Colorado Plateau and the Basin and Range Province. Concomitant with this volcanism, crustal uplift and extension has deformed areas surrounding the Plateau on its east, west, and south sides, while predominantly only elevating the Plateau. Curiously, deformational and magmatic events have left the Colorado Plateau interior relatively unaffected during the entire Phanerozoic Era (Allmendinger and others, 1987).

The Henry and La Sal ranges consist of hypabyssal laccoliths which intrude Mesozoic and late Paleozoic sediments, and which are aligned along north-south trends. Structurally, individual mountains represent discreet intrusive loci comprised of a central stock or laccolith with radial sills and laccoliths. The Henry and La Sal Mountains are composed of five and three intrusive centers, respectively (fig. 2). Nearly 8000 feet of relief is due entirely to intrusive doming and differential erosion. Crystal-bearing magma was emplaced at shallow crustal levels of less than 3-4 km (<1Kbar), based upon generous estimates of the thickness of missing sedimentary section, including a relatively thick Tertiary sequence which may have never been present (Jackson and Pollard, 1988; Hunt, 1958).

Previous investigations (Hunt 1953; 1958; Engel, 1959; Irwin, 1973; Hunt 1988) (M. L. Ross, unpubl. mapping, 1990) indicate that the intrusions are dominantly composed (95%) of plagioclase-hornblende porphyry which typically consists of 20-30% phenocrysts in a typically aphanitic groundmass. Porphyritic-aphanitic Ne-Q normative Na-rich syenite and peralkaline granite were emplaced as stocks, laccoliths, and dikes that cross-cut the plagioclase-hornblende porphyry, and comprise the remainder of the intrusive volume (5%) (M.L. Ross, in prep). Syenitic facies are generally restricted to Mt. Pennell (Henry Mountains) and North Mountain (La Sal Mountains).

Abundant "hornblendite" inclusions (hornblende- and plagioclase-rich rocks) locally comprise 1% of the rocks, and are present in all major intrusive facies. These inclusions include amphibolite-facies gneissic metabasalt xenoliths, probably from the Proterozoic basement, and cognate cumuulate inclusions. The xenoliths are a potential source of an ancient argon component as hornblende xenocrysts in the mineral separates, provided their residence time in the magma was insufficient for complete outgassing of argon.

Previous Age Determinations

The geochronology of the Henry and La Sal Mountains (Stern and others, 1965; Armstrong, 1969; Sullivan, 1987, Sullivan and others, 1991, Dubiel and others, 1990), summarized in figure 3 and table 1, is ambiguous. Stern and others (1965), and Armstrong (1969) reported a bimodal 45-56 and 24-29 Ma age distribution. More recently, Sullivan (1987) and Sullivan and others (1991) determined the ages of 13 samples from the Henry, La Sal, and Abajo Mountains by the fission-track method on sphene and zircon, one of which was concordant with a K-Ar age determination. Their results all fall in the range of 20-30 Ma, suggesting that the K-Ar ages greater than 40 Ma may be in error, and that igneous activity was restricted to near the Oligocene-Miocene boundary. Three recent K-Ar ages by Dubiel and others (1990) also indicate a bimodal age distribution of 25 and 41 Ma (table 1). Clearly there exists some fundamental problem applying either the fission-track or K-Ar technique to these rocks: Either some fission-track ages are too young, or some K-Ar ages are too old.

The Eocene K-Ar ages imply an initial episode of magmatism at 40-56 Ma during Laramide deformation. Shallow subduction seems to have been

present beneath the western US at the latitude of the Henry and La Sal Mountains at this time (e.g. Bird, 1988). This tectonic setting is generally thought to produced a "magmatic gap" (Armstrong. 1974; Cross and Pilger, 1978). However, if igneous activity was entirely Oligocene-Miocene in age, it would suggest that activity in the Henry and La Sal Mountains was related regionally to contemporaneous magmatism in the Reno-Marysvale and San Juan volcanic fields, as suggested by Sullivan and others (1991) and Best (1988).

Fission-Track and K-Ar Ages vs. $^{40}Ar/^{39}Ar$ Ages

Both the K-Ar and fission-track techniques are restricted by assumptions that may affect the accuracy of the results. Fission-track analyses of the Henry and La Sal Mountains have been conducted exclusively on sphene and zircon separates (table 1). Fission-tracks may heal in sphene and zircon, lowering the apparent age, if the rock is at a temperature greater than about 300-400°C for an extended post-crystallization period. For example, given a 1 Ma time interval, fission-tracks in sphene will anneal unless the rock is below 420°C, and will only partially anneal between 420 and 250°C (Naser and Faul, 1969). However, the intrusive porphyries of the Henry and La Sal Mountains are believed to have cooled relatively rapidly, and have suffered no apparent reheating events. Rapid cooling is indicated by the typically porphyritic-aphanitic texture and by the occurrence of cryptically exsolved alkali and ternary feldspars of high structural state ($2t_1 < 0.70$; S. Nelson, unpublished data) in the syenite facies.

There is a paucity of evidence that Eocene intrusions, if present, have been reheated by late Oligocene magmas. Contact metamorphism capable of annealing fission-tracks in the "older" porphyry is conspicuously absent.

Sedimentary screens between intrusive bodies are generally unaltered just a few meters from either intrusive contact. For example, Bull Mountain is a monogenetic intrusion isolated from Mt. Ellen by unaltered Mesozoic country rock, such that the discordant ages (see table 1) cannot be explained by the annealing of fission-tracks by later magmatism or by an elevated ambient geotherm . Despite its improbability in the Colorado Plateau intrusions, the consequences of subsequent reheating by later thermal processes can be detected in $^{40}Ar/^{39}Ar$ release spectra which rise in age with subsequent heating steps (see McDougall and Harrison, 1988) and was considered in this investigation.

Minerals commonly contain excess ^{40}Ar which will result in an apparent K-Ar age that is greater than the true crystallization age. Excess argon in minerals of the Henry and La Sal Mountains intrusions may result from subsolidus diffusion under a high partial pressure of radiogenic Ar (see McDougall and Harrison, 1988). An additional source would be inherited argon from incompletely outgassed older xenocrysts in the magma. Excess argon can be detected by the $^{40}Ar/^{39}Ar$ isochron method (McDougall and Harrison, 1988), but in cases where there are multiple excess argon gradients it may not be possible to unambiguously assign crystallization ages because of the lack of a coherent linear trend(s) in the data (e.g. fig. 5b). However, results from such a sample are still useful: it is possible to constrain a *maximum* age, and recognize that a K-Ar age on such a sample is meaningless. Fortunately, trapped excess argon can occur in one or two discrete components which can be identified with the isochron technique (Heizler and Harrison, 1988) and still give a meaningful crystallization ages (e.g. figs. 4b,c).

The precision of $^{40}Ar/^{39}Ar$ analysis allows the development of a chronology for igneous events closely spaced in time. Furthermore, the

space-time-composition relationships between individual intrusive centers in each mountain range and between both mountains are unknown. Ages reported here utilized the $^{40}Ar/^{39}Ar$ method because it is capable of evaluating pitfalls associated with the other techniques, thereby constraining potentially erroneous ages.

Experimental

analytical

All samples were sized to >100 mesh and separated by standard mineral separation procedures including heavy liquid, magnetic separation, and hand picking techniques to greater than 99% purity. Separates were packaged and irradiated similar to the procedure described by Harrison and Fitz Gerald (1986). Flux monitor FCT-1 (Fish Canyon Tuff sanidine, assumed age of 27.8 Ma) was packaged above, below, and between samples. Two or three individual laser fusions were performed for each flux monitor position, and a J-factor was calculated for each position by weighting the relative proportions of ^{39}Ar released. The J-factors were plotted against sample position, and a second order polynomial was fit to the data ($R^2 \geq 0.999$). This equation was used to calculate the J-factor of each unknown according to its position in the reactor. The error in the J-factor measurement is estimated to be about 0.5%, and was not considered in the regression of isochron data.

Extraction conditions for step heating experiments were also similar to those described by Harrison and Fitz Gerald (1986). Two samples (MW-2 and TUK-1) were analyzed using an automated Nuclide 4.5-60-RSS mass spectrometer. All other samples, including single crystal laser fusions, were analyzed on a VG1200S automated mass spectrometer. Analyses were performed at UCLA, and previous measurements have shown excellent

reproducibility between the two instruments. Errors of all ages reported in tables, figures, text, and the appendix are reported as one standard deviation. Decay constants and isotopic compositions are from Steiger and Jager (1977).

Results

Release spectra in figures 4-10 show the results for individual heating steps assuming an atmospheric trapped component with a $^{40}Ar/^{36}Ar$ ratio of 295.5. The release spectra show the apparent age of each argon fraction versus the cumulative fraction of ^{39}Ar released. Figures 4-10 also include isochron diagrams ($^{39}Ar/^{40}Ar$ versus $^{36}Ar/^{40}Ar$) for all samples analyzed. Crystallization ages were determined from the isochron diagram by the linear regression method described by York (1969) which weights each data point according to its associated uncertainty. The crystallization age is determined by the age equation $t = (1/\lambda)\ln[(^{40}Ar^*/^{39}Ar)J + 1]$, where $^{40}Ar^*/^{39}Ar$ is the inverse of the x-intercept given by linear regression. The composition of the trapped component is given by the inverse of the y-intercept, and values unambiguously less than 0.003384 (corresponding to $^{40}Ar/^{36}Ar > 295.5$) are interpreted to contain excess argon. In some experiments, some of the initial and final steps were omitted in the regression as they were involved release of very non-radiogenic Ar due to degassing of surface adsorbed atmospheric argon or high temperature furnace blanks. Such steps have large analytical uncertainties (≥5%), so that in a weighted regression they have very little influence even if they are included. In addition, some samples had one or more steps which were omitted in linear regression due to large deviations from the apparent isochron(s), and are discussed on a case by case basis below.

Crystallization ages are summarized in table 2. Representative ages are shown in their geologic context in figure 2, and were carefully chosen in order to maximize relative age information. A detailed tabulation of step heating data, and bulk rock chemistry is found in the appendix.

Southern Henry Mountains

Two samples from the southern Henry Mountains were analyzed representing two of the three intrusive centers. No suitable material was available from Mt. Holmes. Mt. Ellsworth is represented by sample ELL-1KRS, and Mt. Hillers by HILL-10KRS.

Mt. Ellsworth

Analytically, ELL-1KRS was an unusual sample. The age spectrum is not flat (fig, 4), and more than 35% of the argon was released during the last heating step (1450 °C), compared to just a few percent or less for most samples (see appendix). Despite the uncertainty of the blank, this step plots near the isochron in figure 4b suggesting the 74.8 Ma age results from incorporation of excess ^{40}Ar. Fifteen steps (3-17, see appendix) were regressed to yield a crystallization age of 31.2 ± 1.0 Ma. Step 18 was also not regressed due to its large deviation from the linear trend of the data. The relatively large error is due in part to the way the data tend to cluster (MSWD = 6.97) instead of being spread out along the isochron. The composition ($^{40}Ar/^{36}Ar$ = 310.8 ± 2.4) of the trapped component in this sample indicates excess argon: Though this value is not vastly different from atmosphere, the low radiogenic yield coupled with the young age explain the scatter in the release spectrum, and the observation that the apparent age of all heating steps exceeds the crystallization age. ELLN-1KRS exemplifies the effect of excess argon as K-Ar

analysis would give an age significantly older than the crystallization age given here.

Mt. Hillers

HILL-10KRS also contained excess argon, but in two distinct components, the release of which appears to be thermally controlled: This is a phenomenon that has been reported before (see Heizler and Harrison, 1988). The fact that there appears to be two distinct linear trends on the isochron diagram, and that they regress to give nearly identical ages is probably not fortuitous in light of the ages being geologically meaningful. This also accounts for the lack of a flat age spectrum for this sample (fig.4a). Steps 1-7 lie along an isochron with an age of 29.1 ± 0.3 Ma ($^{40}Ar/^{36}Ar$ = 316.8 ± 9.9). Steps 9-12 also lie along an isochron with an age of 29.6 ± 0.4 Ma and a trapped component of $^{40}Ar/^{36}Ar$ = 464 ± 11. In all, 4 steps were omitted in the linear regression analyses. In addition to the non-radiogenic first step, step 16 plots well away from both trends and was also excluded. The two steps that fall between the trends may represent mixing between these two components and were also excluded. We interpret a crystallization age for this sample of 29.4 ± 0.3 Ma. Even if it is assumed that there is no correlation on the isochron diagram, step heating results constrain the maximum age of this sample to less than 30 Ma.

Dubiel and others (1990) report a hornblende K-Ar age of 24.8 ± 2 Ma (table 1) for a separate laccolithic body at Mt. Hillers. This age is an average of three discordant analyses at 20.4 ± 2, 26 ± 0.7, and 28 ± 0.5 Ma (S. Church, personal communication, 1991). All of these ages are at least 1 Ma younger than our determination for Hill-10KRS. It is therefore possible that igneous activity may have proceeded for an extended period of time at Mt. Hillers.

Additional $^{40}Ar/^{39}Ar$ age determinations are necessary to confirm this conclusion.

Northern Henry Mountains

Mt. Ellen

Mt. Ellen is represented by three samples, ELLN-4, ELLN-10, and BULL-1. Our BULL-1 is from the same intrusive body as BULL-1 (Sullivan and others, 1991) and sample 751 (Armstrong, 1969). This provides a check on discordant K-Ar and fission track age determinations (table 1).

ELLN-4 has a complex age spectrum and scattered isochron plot (fig. 5a,b). The apparent plateau at approximately 66 Ma is geologically meaningless, and is the result of one heating step, only a 10 °C increment over the previous step, for which nearly 70% of the gas was released. Figure 5b shows that the gas was very heterogeneous in composition, and no crystallization age can be determined for this sample. The crystallization age must be younger than the youngest apparent age for a reliable heating step. Step 2 has an age of 35.7 Ma, and the crystallization age of this sample must be less than this, although there is no way to constrain how much less by our $^{40}Ar/^{39}Ar$ data alone. Note, that a conventional K-Ar age on this sample would greatly over-estimate its crystallization age.

ELLN-10 has a relatively flat age spectrum (fig. 5a) and the isochron (fig. 5c) defines a reasonably good array, but has scatter about it greater than the uncertainty in the measurements (MSWD = 173). We suggest that the scatter may result from a non uniform trapped argon component. The data regress to a crystallization age of 29.4 ± 0.3 Ma and a $^{40}Ar/^{36}Ar$ ratio of 320 ± 15.

Bull-1 also has a complicated age spectrum and isochron diagram (fig. 5a,d) due to the effects of heterogeneous excess argon. Nonetheless, steps 7-10

form a small plateau that constrains a maximum age for the sample of about 34 Ma, much younger than Armstrong's (1969) age of 44.8 Ma (table 1). In fact, the total gas age for this sample is 44.6 Ma. We believe the fission-track age of 28.6 ± 1.2 Ma (Sullivan and others, 1991) to be the best estimate of the crystallization age of this intrusion.

Mt. Pennell

Six samples from Mt Pennell were analyzed in order to determine the relative and isotopic ages of the plagioclase-hornblende porphyry (ELLN-7, PENL-14, and PENL-13) and the younger, cross-cutting syenitic facies (PENL-3, PENL-9, and PENL-12).

ELLN-7 has a complicated age spectrum and isochron plot that are difficult to interpret (fig. 6a,b). The total gas age for this sample is 43.2 Ma, and the youngest apparent age on the release spectrum suggests that the sample is less than about 28 Ma. Single crystal laser fusion results (fig. 6b) define an isochron with an age of 23.3 ± 0.2 Ma. This is concordant with the zircon fission-track age of this intrusion of 23.9 ± 1.1 Ma (table 1; sample PENL-1). We believe the failure to produce an isochron by step heating of bulk mineral separates in this and other samples described in this study indicates the presence of incompletely outgassed xenocrysts in the rock.

Steps 4-15 for PENL-14 form a roughly linear trend (MSWD = 148.4) in figure 6c, and regress to give an age of 22.5 ± 1.9 Ma, with considerable excess argon ($^{40}Ar/^{36}Ar$ = 690 ± 51) (fig. 6c). PENL-13 has a flat age spectrum and well correlated isochron (fig. 7). Steps 3-17, which comprise 90% of the total gas, yield a well constrained crystallization age of 24.9 ± 0.1 Ma and atmospheric $^{40}Ar/^{36}Ar$ (293.1 ± 1.7). We interpret this age to be the best estimate of the plagioclase-hornblende porphyry.

The material analyzed for PENL-9 was a cryptically exsolved alkali feldspar, whereas PENL-12 and PENL-3 were, respectively, hornblende separates from syenite porphyry and a cumulate hornblende + clinopyroxene + apatite + magnetite inclusion in syenite. All three samples yield flat age spectra and linear isochron plots (figure 8). $^{40}Ar/^{36}Ar$ ratios are within 2 standard deviations of atmosphere, and the samples have nearly identical ages ranging between 24.4-25.4 Ma (see figs. 8b-d and appendix for details). Steps 9 and 10 were omitted from the regression for PENL-3 due to obvious deviation from the isochron. Including them in the data set give an apparent age significantly younger than their host porphyry. It appears that all the Mt. Pennell rocks were emplaced at about 25 Ma, with no resolvable age difference between the intrusive facies except for ELLN-7 which is not constrained by cross-cutting relationships. Figure 8a illustrates this by comparing the release spectra of syenite porphyry (PENL-3, 9, 12) and plagioclase-hornblende porphyry (PENL-13). Thus the cross-cutting relationships would seem to also constrain the age of PENL-14 to greater than 25 Ma, although this value is well within two standard deviations of our reported crystallization age.

La Sal Mountains

Six samples were analyzed from the La Sal Mountains. Three hornblende separates (MW-13, TUK-2, TUK-6) represent plagioclase-hornblende porphyry from North, Middle, and South Mountains respectively. Two alkali feldspar separates represent a syenite porphyry stock (MW-2) and a younger syenite porphyry dike (MW-17) from North Mountain, while another alkali feldspar separate (TUK-1) represents a syenite porphyry laccolith from Middle Mountain.

Step heating experiments reveal the existence of significant sample heterogeneity in the form of incompletely outgassed xenocrysts in the hornblende separates (fig. 9). Evidence for this is reflected in ages of individual steps that exceed the age of the country rock, and the complete lack of correlation in the isochron diagrams. Single crystal laser experiments on all three plagioclase-hornblende porphyry samples demonstrate the existence of late Oligocene magmatic hornblende in addition to xenocrystic components (see table 2; appendix 1a).

North Mountain

Mw-17 is considered the youngest of the North Mountain samples on the basis of cross-cutting relationships (M. L. Ross, unpubl. mapping, 1990). It represents a late Ne-normative syenite dike which cuts across much of the intrusion. MW-17 has a flat age spectrum, especially for steps 15-19 which represent 40% of the gas (fig. 10a). These steps regress to give an age of 27.9 ± 0.03 Ma with atmospheric argon ($^{40}Ar/^{36}Ar = 296.7 \pm 5$) and MSWD < 1 (fig. 10b). Regression of steps 5-19, which includes all but the final and 4 initial non-radiogenic steps, gives an identical age, but with a much larger uncertainty (0.3 Ma), MSWD (31.5), and may include a component of excess argon ($^{40}Ar/^{36}Ar = 342 \pm 11$) that was exhausted at higher temperatures (fig. 10b).

MW-2 has a flat age spectrum (fig. 11a) and associated crystallization age of 27.9 ± 0.3 Ma and atmospheric trapped argon ($^{40}Ar/^{36}Ar = 302 \pm 10$). Some of the scatter in the isochron diagram (fig. 11b) is a result of small gas fractions analyzed on the relatively insensitive Nuclide spectrometer. MW-2 represents a peralkaline syenite stock that is intermediate in age to MW-17 and the plagioclase-hornblende porphyry at North Mountain (MW-13).

Cross-cutting relationships, and comparison of step heating results constrain the age of MW-13 to between 27.9 ± 0.3 and 31.5 ± 1.4 Ma. This agrees with fission track ages on North Mountain plagioclase-hornblende porphyry of 28.7 ± 1.4 (zircon) and 30.3 ± 1.6 (sphene) Ma (table 1; sample CSTV-2). Single crystal laser fusions of MW-13 support the conclusion that the uncorrelated isochron plots are the result of xenocrystic hornblende. Table 2 summarizes those results as reported in appendix 1a. The five analyzed crystals range in apparent age from 82.8 to 26.5 Ma, indicating strong sample heterogeneity. However, three of the five crystals give concordant late Oligocene ages with a mean value of 27.5 ± 1.4 Ma. MW-13 must exceed 27.9 Ma given that this intrusion is cut by two well-constrained samples of that age. We interpret the remaining crystals as representing partially outgassed xenocrysts which may have magmatic overgrowths.

Middle Mountain

TUK-1 alkali feldspar is from a Ne-normative syenite porphyry sill sampled from the middle La Sal Mountains. It has a relatively flat age spectrum and somewhat scattered isochron plot (fig. 12a,b), but with relatively low precision due to the Nuclide mass spectrometer. The isochron suggests a crystallization age of 26.7 ± 0.2 Ma ($^{40}Ar/^{36}Ar = 285 \pm 6$) regressed for all steps. Sullivan and others' (1991) age for this sample (28.5 ± 1.9 Ma; see table 1, sample LAS-1).is concordant with our determination.

Step heating experiments on TUK-2 (fig. 9a,c) reveal little useful information other than the presence of inherited argon and a maximum crystallization age of 62.9 Ma. Laser fusions of 13 crystals also indicate sample heterogeneity, with 9 of them giving late oligocene-earliest Miocene ages that have a mean of 25.1 ± 4.1 Ma (table 2; appendix 1a). The scatter in these 9

apparent ages may be due in part to the low intensity of the ^{36}Ar peak height for many of the crystals relative to the ^{36}Ar blank, leading to large uncertainties in the $^{40}Ar/^{36}Ar$ ratios.

South Mountain

Step heating data for TUK-6 are generally not useful except to indicate a maximum crystallization age of 56.5 Ma. Similar to samples MW-13 and TUK-2, TUK-6 also shows sample heterogeneity in laser fusion experiments. Crystals have apparent ages up 231.4 Ma. Two of the five crystals analyzed have late Oligocene ages with a mean of 26 ± 2.6 Ma

Discussion

The most obvious result of this study is that none of the intrusive rocks of the Henry and La Sal Mountains are older than 32 Ma (fig. 3). We believe that previously determined K-Ar ages greater than this are almost certainly affected by excess argon (e.g. ELLN-1KRS, HILL-10KRS, and PENL-14) or by xenocrysts (e.g. ELLN-4, ELLN-7, BULL-1, MW-13, TUK-2, and TUK-6) in the sample. This study also generally corroborates the relative validity of recent fission-track work (Sullivan and others, 1991). However, we have not found any samples as young as fission-track ages of 20 Ma, as none of our samples are unambiguously younger than about 23.3 Ma. In general, the fission-track ages all have relatively large uncertainties, and some of the youngest ages show significant internal discordance between sphene and zircon determinations (table 1).

The lack of an Eocene magmatic component indicates that igneous activity in the Henry and La Sal Mountains did not occur in two distinct

tectonic settings and time periods. Our results help affirm the validity of Armstrong's (1974) "magmatic gap", as previous Eocene K-Ar ages were exceptions to his observation. The fact that magmatism appears to have been limited to the late Oligocene also supports the concept of an east-west Reno-San Juan magmatic belt as proposed by Best (1988) and Sullivan and others, (1991)

Henry Mountains

Magmatism in the Henry Mountains appears to have been active over several million years (31.2-23.3 Ma). It may have been initiated at Mt Ellen and Mt. Ellsworth at the extreme ends of the range, and culminated with magmatism at Mt. Pennell, although data from Mt. Hillers suggest that this apparent progression of ages may reflect incomplete sampling of relatively long-lived magmatic loci.

The results from Mt Pennell indicate that emplacement of undersaturated syenitic magmas followed the emplacement of metaluminous plagioclase-hornblende porphryry within the resolution of the technique, and that weak mineralization associated with syenitic magmatism can be placed at about 25 Ma. However, the Horn Laccolith (Hunt, 1958), a slightly peraluminous silica-rich satellite intrusion of plagioclase-hornblende porphyry (sample ELLN-7; appendix 1b) north of Mt Pennell, appears to be younger than the syenite porphyry. This chemically and petrographically distinct intrusion may represent a late-stage differentiate of the igneous system. In addition, the presence of xenocrysts in this sample as the source of the heterogeneous excess argon seen in step heating experiments (fig. 6b), is a probable explanation for similar results in other

samples from both ranges. Thus, the assimilation of crustal material should be addressed in any geochemical evaluation of these rocks.

Data from individual laccoliths at Mt. Hillers and Mt Pennell indicate that magmatism may have been active at individual intrusive centers for periods of time in excess of 2 Ma. This is consistent with mapping and field observations which show that the individual intrusive centers are comprised of petrographically distinct and variably evolved multiple laccoliths.

La Sal Mountains

Igneous activity in the La Sal Mountains may range over a smaller time-span (25.1-27.9 Ma) than the Henry Mountains. It appears that the entire igneous episode at North Mountain occurred at about 27.9 Ma. Late, unmineralized cross-cutting dikes, and slightly older ore deposition associated with emplacement of the Mineral Mountain syenite (MW-2) appear to have occurred at 27.9 Ma,.and affected plagioclase-hornblende porphryry of about the same age. Hornblende separates from plagioclase-hornblende porphryry of all three intrusive centers contain xenocrysts, although single crystal experiments confirm the presence of magmatic (late Oligocene) hornblende in each of them.

Acknowledgements

We thank Mark Harrison for the use of his lab facilities and thoughtful input. Myron Best of Brigham Young University and John Obradovitch of the USGS provided thoughtful reviews of the manuscript. This project was generously supported by the Utah Geological and Mineral Survey, whose staff

has taken an active and supportive interest in this research. Supported was also provided by NSF grant EAR 8915780.

References Cited

Allmendinger, R.W., Hauge, T.A., Hauser, E.C., Potter, D.J., Klemperer, S.L., Nelson, K.D., Kneupfer, P. and Oliver, J., 1987, Overview of the COCORP 40°N transect, western United States: The fabric of an orogenic belt: Bulletin of the Geological Society of America, v. 98, p. 308-319.

Armstrong, R.L., 1969, K-Ar dating of laccolithic centers of the Colorado Plateau and vicinity: Geological Society of America Bulletin v. 80, p. 2081-2086.

Armstrong, R.L., 1974, Magmatism, orogenic timing, and orogenic diachronism in the Cordillera from Mexico to Canada: Nature, v. 247, P. 348-351.

Bennett, V.C., and DePaolo, D.J., 1987, Proterozoic crustal history of the western United States as determined by neodymium isotopic mapping: Geological Society of America Bulletin, v. 99, p. 674-685.

Best, M.G., 1988, Early Miocene change in direction of least principle stress, southwestern United States: Conflicting inferences from dikes and metamorphic core-detachment fault terranes: Tectonics, v. 7, p. 249-259

Bird, P., 1988, Formation of the Rocky Mountains, western United States: A continuum computer model: Science, v. 239, p. 1501-1507.

Burke, D.B., and McKee, E.H., 1979, Mid Cenozoic volcano-tectonic troughs in central Nevada: Bulletin of the Geological Society of America, v. 90, p. 181-184.

Not found in text.

Cross, T.A., and Pilger, R.H., 1978, Constraints on absolute motion and plate interaction inferred from Cenozoic igneous activity in the western United States: American Journal of Science, v. 278, p. 865-902.

Dubiel, R.F., Bromfield, C.S., Church, S.E., Kemp, W.M., Larson, M.J., Peterson, F., and Pierson, C.T., 1990, Mineral resources of the Mount Pennell wilderness study area, Garfield County, Utah: United States Geological Survey Bulletin 1751D, p. D1-D17.

Engel, C., 1959, Igneous rocks and constituent hornblendes of the Henry Mountains, Utah: Geological Society of America Bulletin, v. 70, p. 961-980.

Harrison, T.M., and Fitz Gerald, J.D., 1986, Exsolution in hornblende and its consequences for $^{40}Ar/^{39}Ar$ age spectra and closure temperature: Geochimica et Cosmochemica Acta, v. 50, p. 247-253.

Heizler, M.T., and Harrison, T.M., 1988, Multiple trapped argon isotope components revealed by $^{40}Ar/^{39}Ar$ isochron analysis: Geochimica et Cosmochemica Acta, v. 52, p. 1295-1303.

Hunt, C.B., 1953, Geology and geography of the Henry Mountains region, Utah: U.S. Geological Survey Professional Survey Paper 228, 234 p.

Hunt, C.B., 1958, Structural and igneous geology of the La Sal Mountains, Utah: U.S. Geological Survey Professional Paper 294-I p. 305-394.

Hunt, G.L., 1988, Petrology of the Mt. Pennell central stock, Henry Mountains, Utah: Brigham Young University Geology Studies, v. 35, p. 81-100.

Irwin, T.D., 1973, The petrologic evolution of the North Mountains Stock, La Sal Mountains, Utah: unpublished masters thesis, University of Arizona, 71 p.

Jackson, M.D., and Pollard, D.D., 1988, The laccolith-stock controversy: new results from the southern Henry Mountains, Utah: Geological Society of America Bulletin, v. 100, p. 117-139.

Karlstrom, K.E., Bowring, S.A., and Conway, C.M., 1987, Tectonic significance of an Early Proterozoic two-province boundary in central Arizona: Geological Society of America Bulletin, v. 99, p. 529-538.

McDougall, I., and Harrison, T.M., 1988, Geochronology and Thermochronology by the $^{40}Ar/^{39}Ar$ Method. Oxford University Press. New York.

Naeser, C.W., and Faul, H., 1969, Fission-track annealing in apatite and sphene: Journal of Geophysical Research, v. 74, p. 705-710.

Ross, M.L., in prep., Geologic map of the Mt. Waas quadrangle, Grand County, Utah: Utah Geological Survey.

Steiger, R.H., and Jager, E., 1977, Subcommission on geochronology: Convention on the use of constants in geo- and cosmochronology: Earth and Planetary Science Letters, v. 36, p. 359-362.

Stern, T.W., Newell, M.F., Kistler, R.W., and Shawe, D.R., 1965, Zircon uranium-lead and thorium-lead ages and mineral potassium-argon ages of La Sal Mountains rocks, Utah: Journal of Geophysical Research, v. 70, p. 1503-1507.

Sullivan, K.R., 1987, Igneous intrusions in southeastern Utah: Relation to space-time-composition patterns of Cenozoic igneous activity in Nevada,Utah, and Colorado: Geological Society of America Abstracts with Programs, v. 19, p. 337.

Sullivan, K.R., Kowallis, B.J., and Mehnert, H.H., 1991, Isotopic ages of igneous intrusions in southeastern Utah: evidence for a mid-Cenozoic Reno-San Juan Magmatic Zone: Brigham Young University Geology Studies, v. 37, in press.

Thompson, G.A., and Zoback, M.L., 1979, Regional geophysics of the Colorado Plateau: Tectonphysics, v. 61, p. 149-181.

York, D., 1969, Least squares fitting of a straight line with correlated errors: Earth and Planetary Science Letters, v. 5, p. 320-324.

FIGURE CAPTIONS

Figure 1. Index map showing the location of the Henry and La Sal Mountains and their regional relationship to tectono-magmatic elements in the western U.S.

Figure 2. Generalized geologic maps of a) the Henry Mountains, and b) the La Sal Mountains. Selected ages are given to illustrate time-space relationships for the intrusive rocks.

Figure 3. Histogram of isotopic age determinations for intrusive rocks of the Henry and La Sal Mountains. Note that all Eocene age determinations were by the K-Ar method, and are interpreted to be the result of excess argon and partially outgassed hornblende xenocrysts in samples that are actually late-Oliogcene in age.

Figure 4. a) Release spectra for samples ELL-1KRS, and HILL-10KRS representing Mt Ellsworth, and Mt Hillers respectively. Neither sample has a flat release spectrum due in part to excess argon. b) Isochron diagram for ELL-1KRS. c) Isochron diagram for HILL-10KRS showing two distinct trapped argon components which regress to give nearly identical ages. Solid symbols in this and all subsequent figures indicate data points omitted in linear regression to determine the crystallization age.

Figure 5. a) Release spectra for samples ELLN-4, ELLN-10, BULL-1 from Mt Ellen. b) Isochron diagram for ELLN-4 shows no linear trend which we believe to be the result of xenocrysts, or inherited argon. c) Isochron diagram and

accompanying crystallization age for ELLN-10. d) Isochron diagram for Bull-1 indicating inherited argon.

Figure 6. a) Release spectra for samples ELLN-7 and PENL-14 from Mt. Pennell. b) Isochron diagram for ELLN-7. Circles indicate the results of single crystal laser fusions which clearly define an isochron, while squares indicate data influenced by inherited argon revealed by step-heating experiments. We believe this sample strongly indicates that compositionally heterogeneous argon is due to the presence of xenocrysts in the sample. c) Isochron diagram for Penl-14.

Figure 7. a) Flat release spectrum and b) isochron diagram for PENL-13 from Mt. Pennell.

Figure 8. a) Flat release spectra for syenitic rocks (PENL-3, PENL-9, and PENL-12) from Mt. Pennell compared with plagioclase-hornblende porphyry (PENL-13) that they cross-cut. Note that these samples are essentially the same age implying that the emplacement of both facies was essentially contemporaneous. Isochron diagrams are for b) PENL-3, c) PENL-9, and d) PENL-12.

Figure 9. a) Complex release spectra for MW-13, TUK-2, and TUK-6 representing plagioclase-hornblende porphyry from North, Middle, and South Mountains respectively. Note that some steps give ages that are significantly older than Cretaceous country rock cut by the intrusions, another evidence of inherited argon in these samples. Isochron diagrams for b) MW-13, c) TUK-2, and d) TUK-6.

Figure 10. a) Release spectrum for syenite porphyry dike (MW-17) from North Mountain and b) associated isochron diagram. Inclusion of the deleted points has little effect on the crystallization age.

Figure 11. a) Release spectrum for syenite porphyry stock (MW-2) from North Mountain and b) associated isochron diagram.

Figure 12. a) Release spectrum for syenite porphyry laccolith (TUK-1) from Middle Mountain and b) associated isochron diagram.

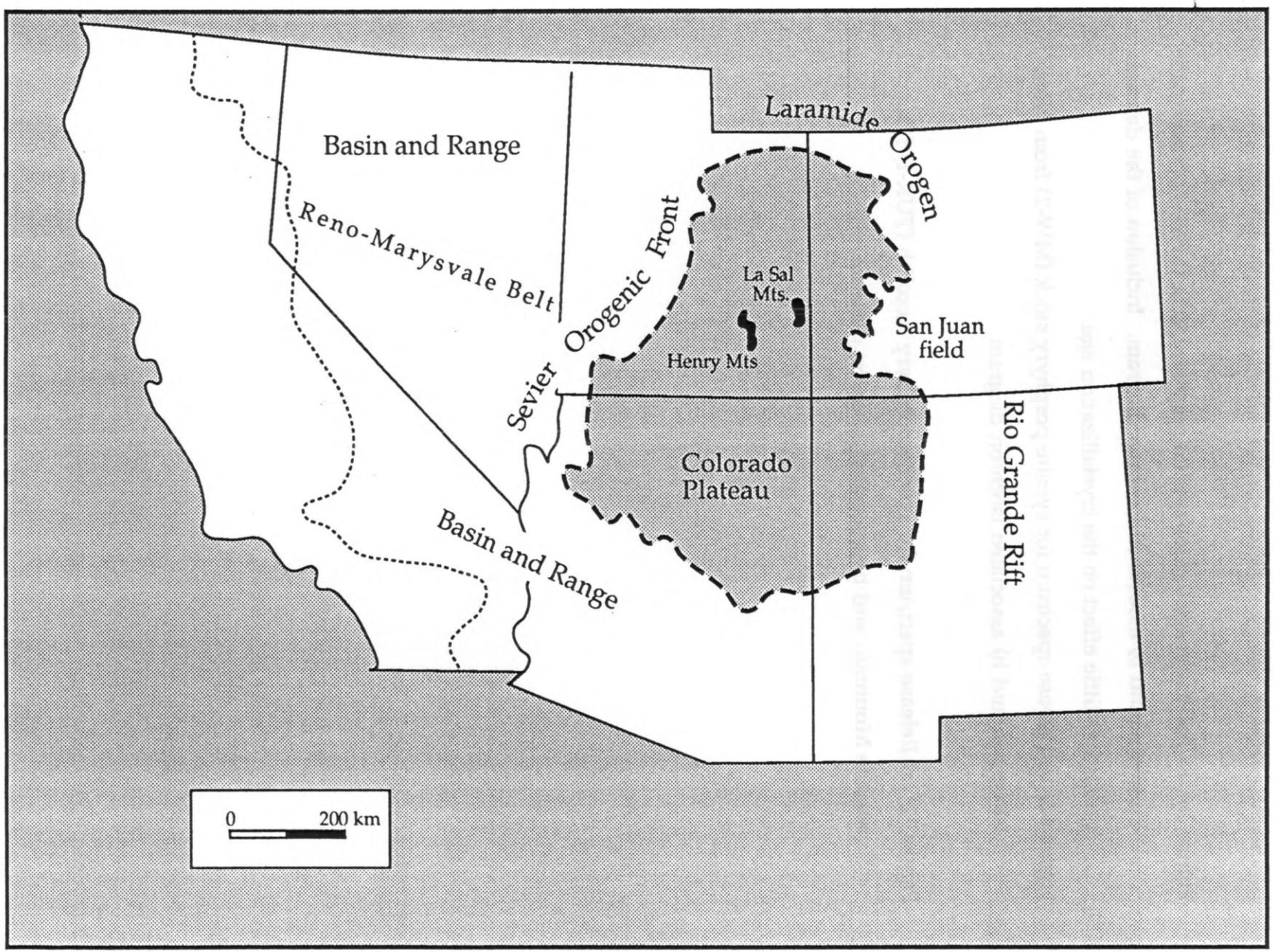
Basin and Range
Reno-Marysvale Belt
Laramide
Orogen
Sevier Orogenic Front
La Sal
Mts.
Henry Mts
San Juan
field
Colorado
Plateau
Rio Grande Rift
Basin and Range
0
200 km

FIGURE 1.

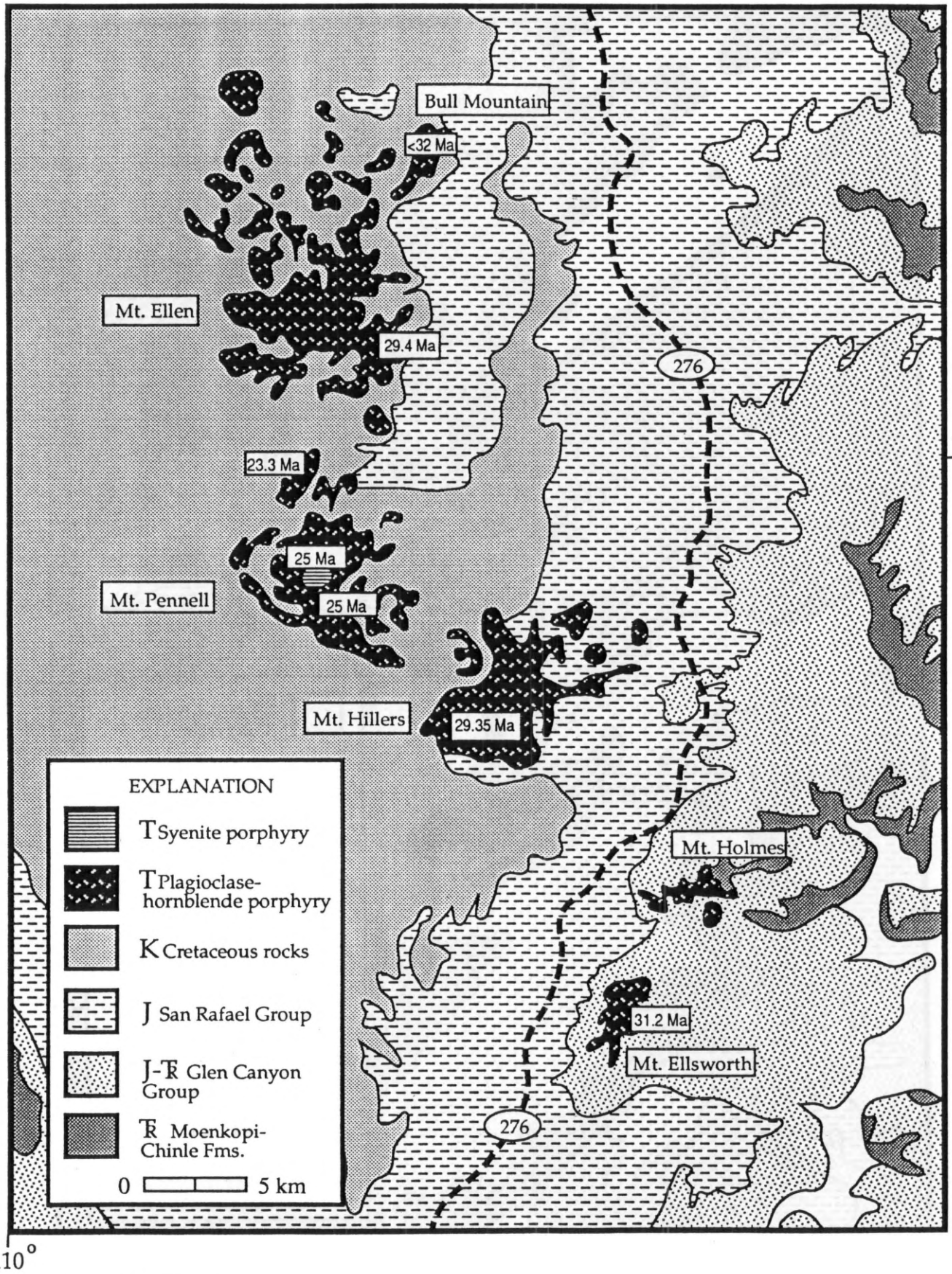
Bull Mountain
<32 Ma
Mt. Ellen
29.4 Ma
276
23.3 Ma
25 Ma
Mt. Pennell
25 Ma
Mt. Hillers
29.35 Ma
Mt. Holmes
31.2 Ma
Mt. Ellsworth
276
38°
110°
EXPLANATION
T Syenite porphyry
T Plagioclase-hornblende porphyry
K Cretaceous rocks
J San Rafael Group
J-Tr Glen Canyon Group
Tr Moenkopi-Chinle Fms.
0
5 km

FIGURE 2a.

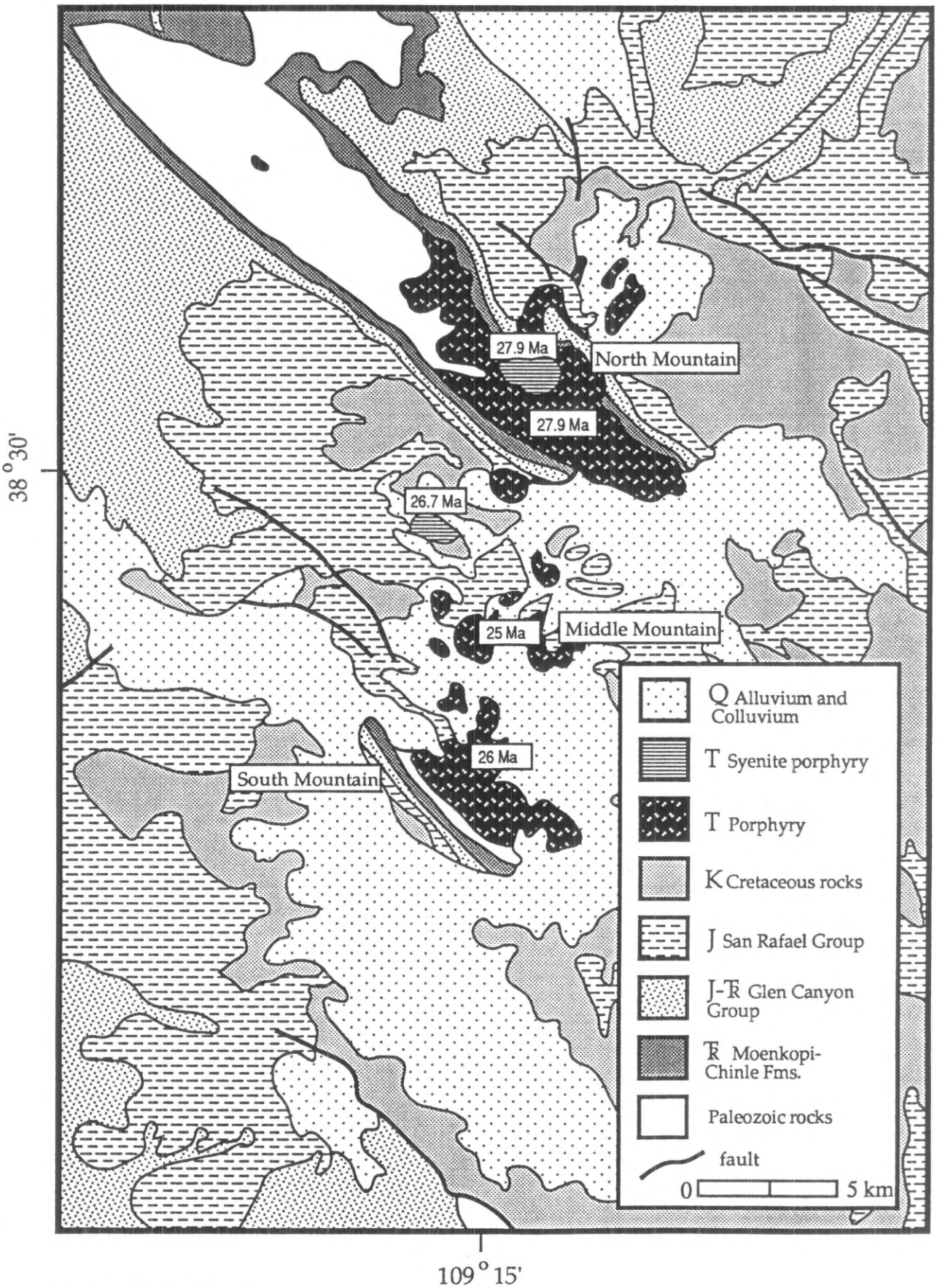
27.9 Ma
North Mountain
27.9 Ma
26.7 Ma
25 Ma
Middle Mountain
26 Ma
South Mountain
Q Alluvium and Colluvium
T Syenite porphyry
T Porphyry
K Cretaceous rocks
J San Rafael Group
J-TR Glen Canyon Group
TR Moenkopi-Chinle Fms.
Paleozoic rocks
fault
0
5 km
38°30'
109°15'

FIGURE 2b.

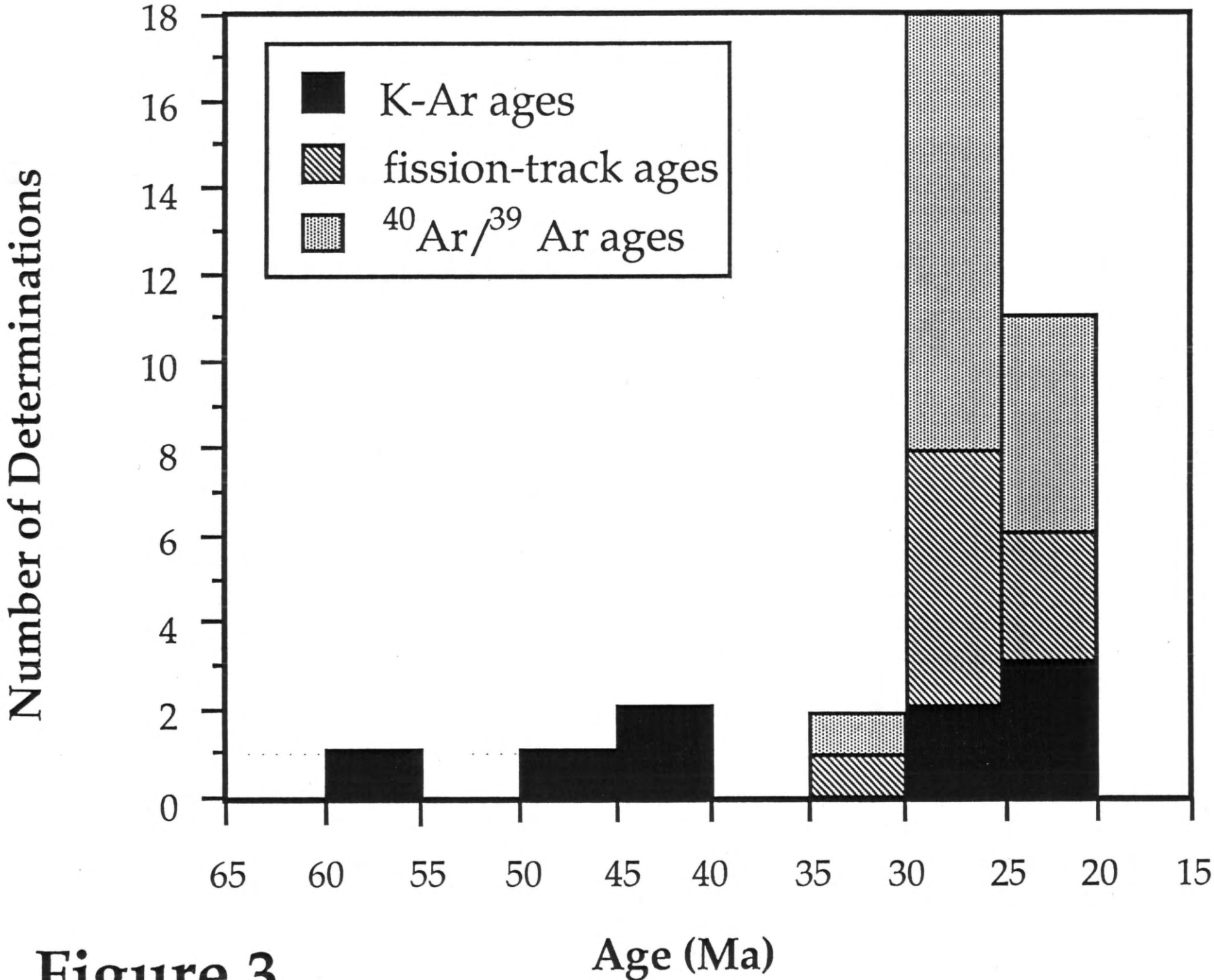
K-Ar ages
fission-track ages
40Ar/39 Ar ages
Number of Determinations
0
2
4
6
8
10
12
14
16
18
65
60
55
50
45
40
35
30
25
20
15
Age (Ma)

Figure 3.

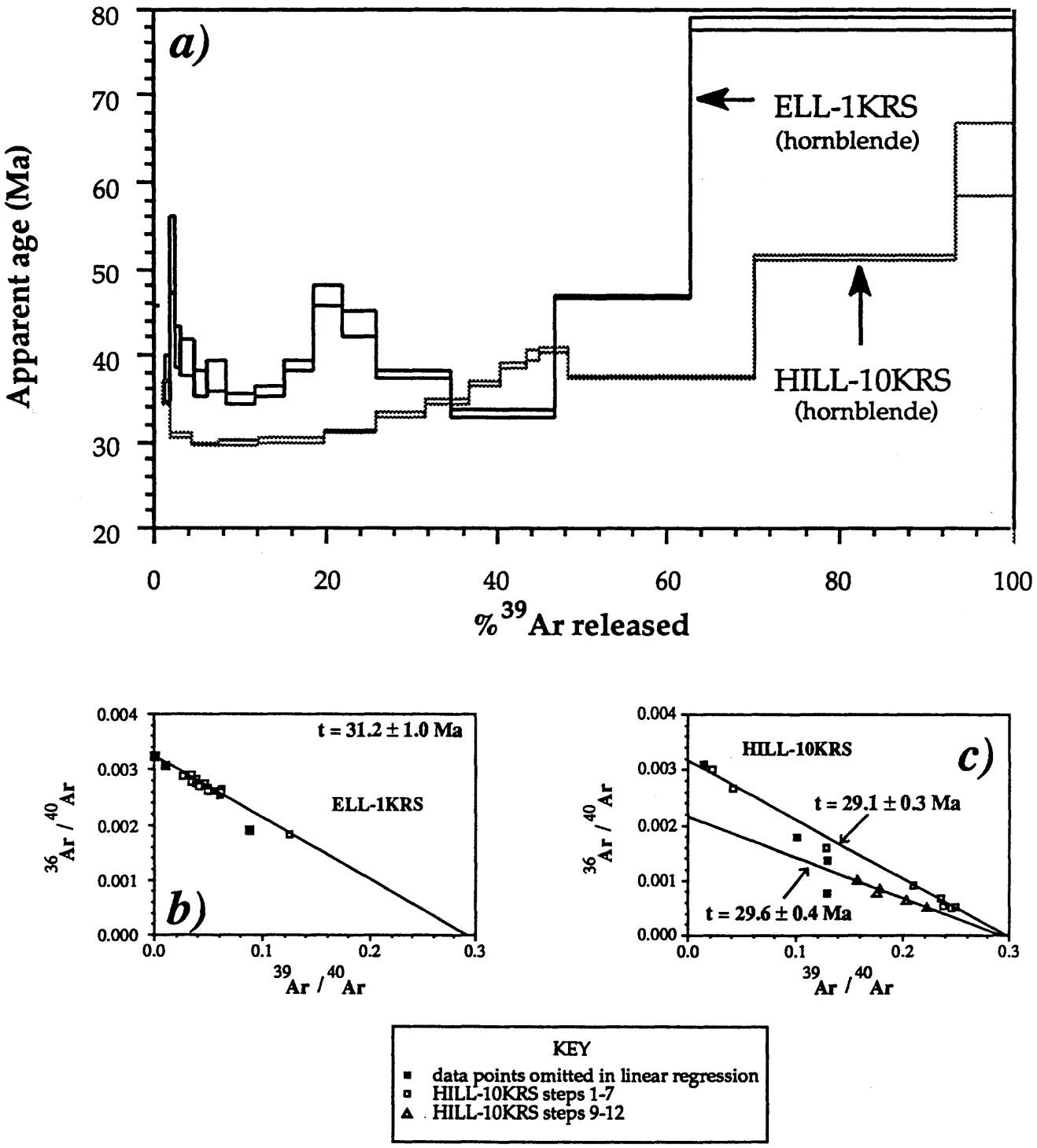
a)
ELL-1KRS
(hornblende)
HILL-10KRS
(hornblende)
Apparent age (Ma)
%39Ar released
b)
t = 31.2 ± 1.0 Ma
ELL-1KRS
36Ar / 40Ar
39Ar / 40Ar
c)
HILL-10KRS
t = 29.1 ± 0.3 Ma
t = 29.6 ± 0.4 Ma
KEY
data points omitted in linear regression
HILL-10KRS steps 1-7
HILL-10KRS steps 9-12

Figure 4.

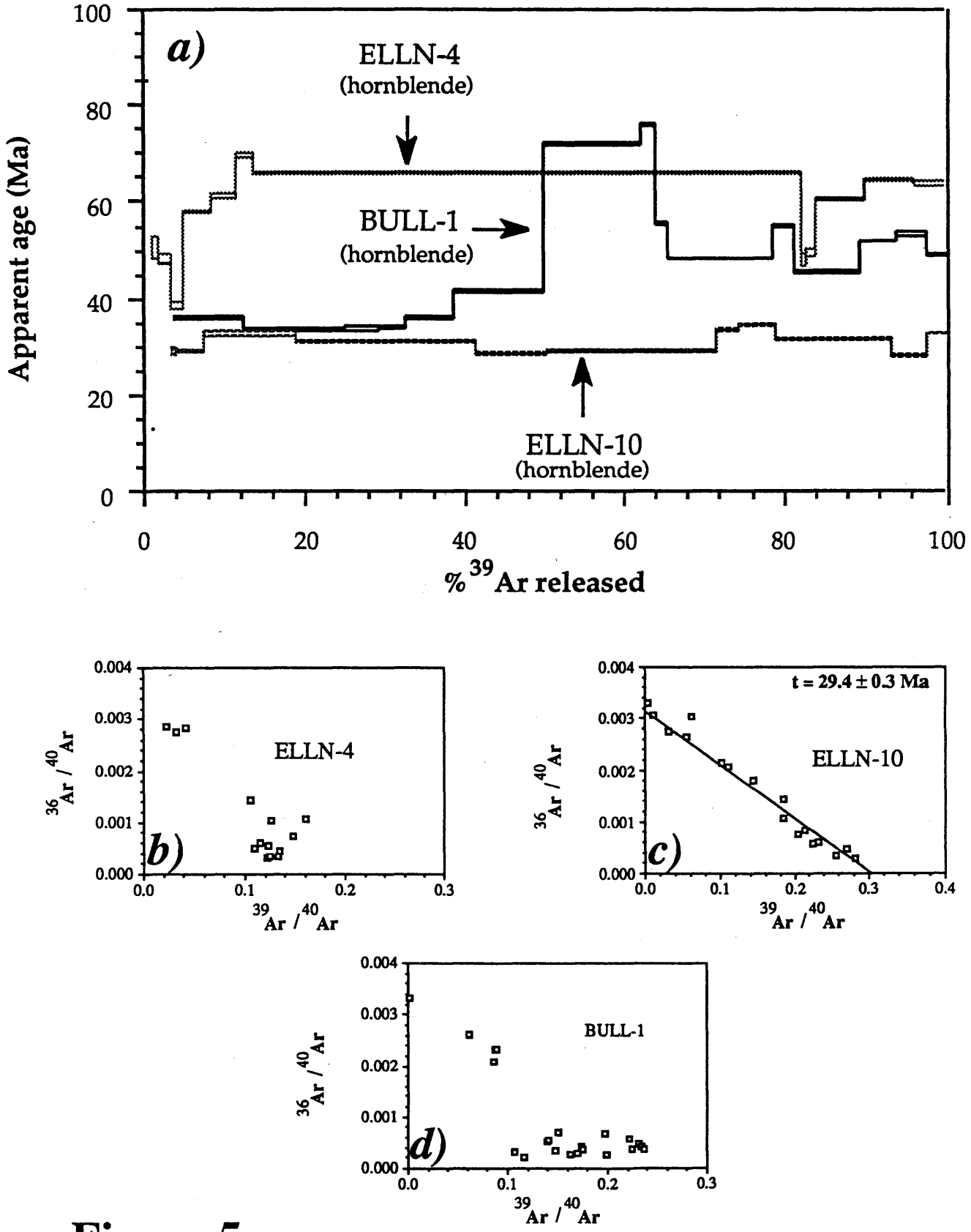
a)
ELLN-4
(hornblende)
BULL-1
(hornblende)
ELLN-10
(hornblende)
Apparent age (Ma)
% 39Ar released
b)
ELLN-4
c)
t = 29.4 ± 0.3 Ma
ELLN-10
d)
BULL-1
36Ar / 40Ar
39Ar / 40Ar

Figure 5.

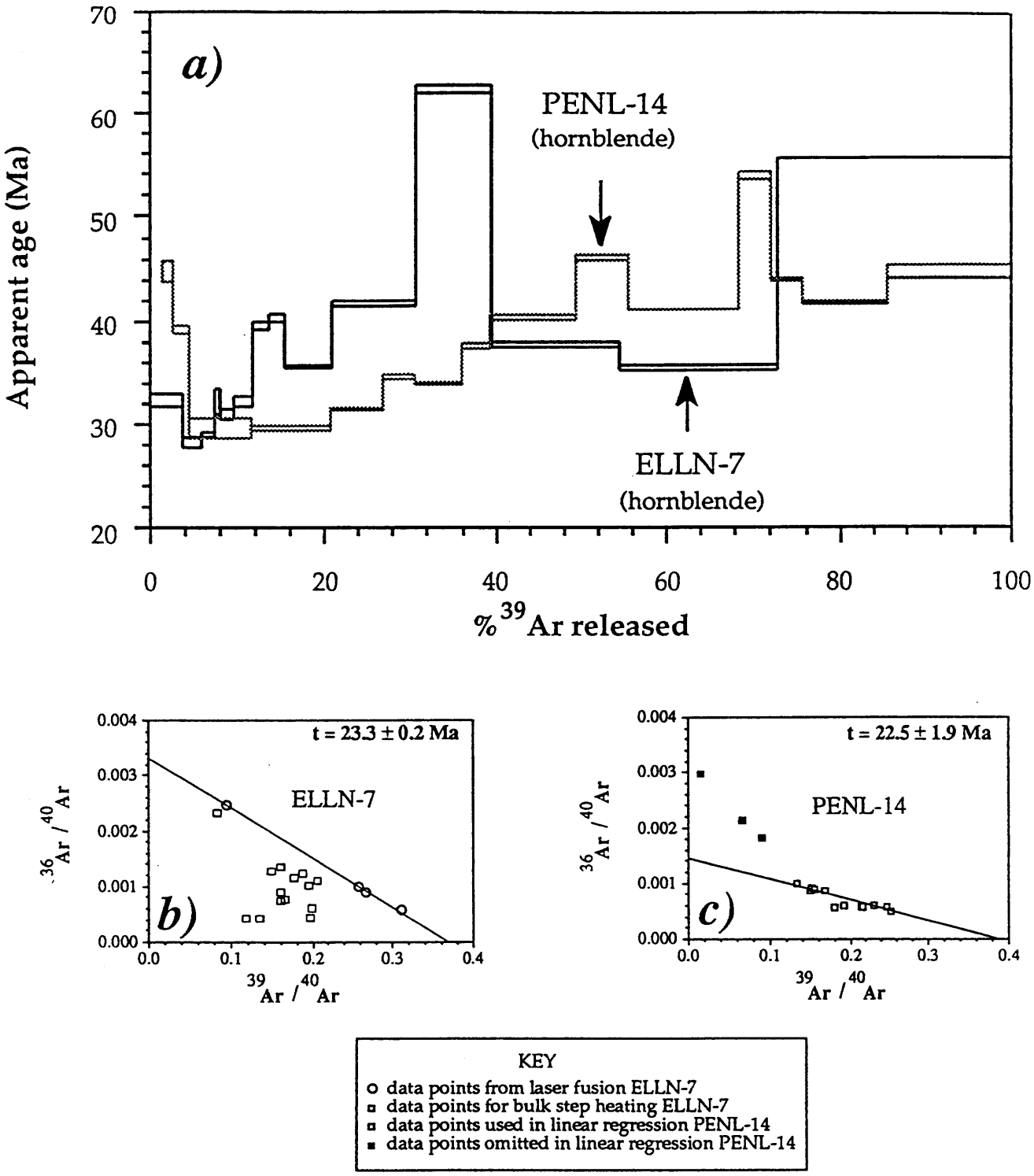
a)
PENL-14
(hornblende)
ELLN-7
(hornblende)
Apparent age (Ma)
70
60
50
40
30
20
0
20
40
60
80
100
% 39Ar released
b)
t = 23.3 ± 0.2 Ma
ELLN-7
36Ar / 40Ar
39Ar / 40Ar
0.004
0.003
0.002
0.001
0.000
0.0
0.1
0.2
0.3
0.4
c)
t = 22.5 ± 1.9 Ma
PENL-14
KEY
data points from laser fusion ELLN-7
data points for bulk step heating ELLN-7
data points used in linear regression PENL-14
data points omitted in linear regression PENL-14

Figure 6.

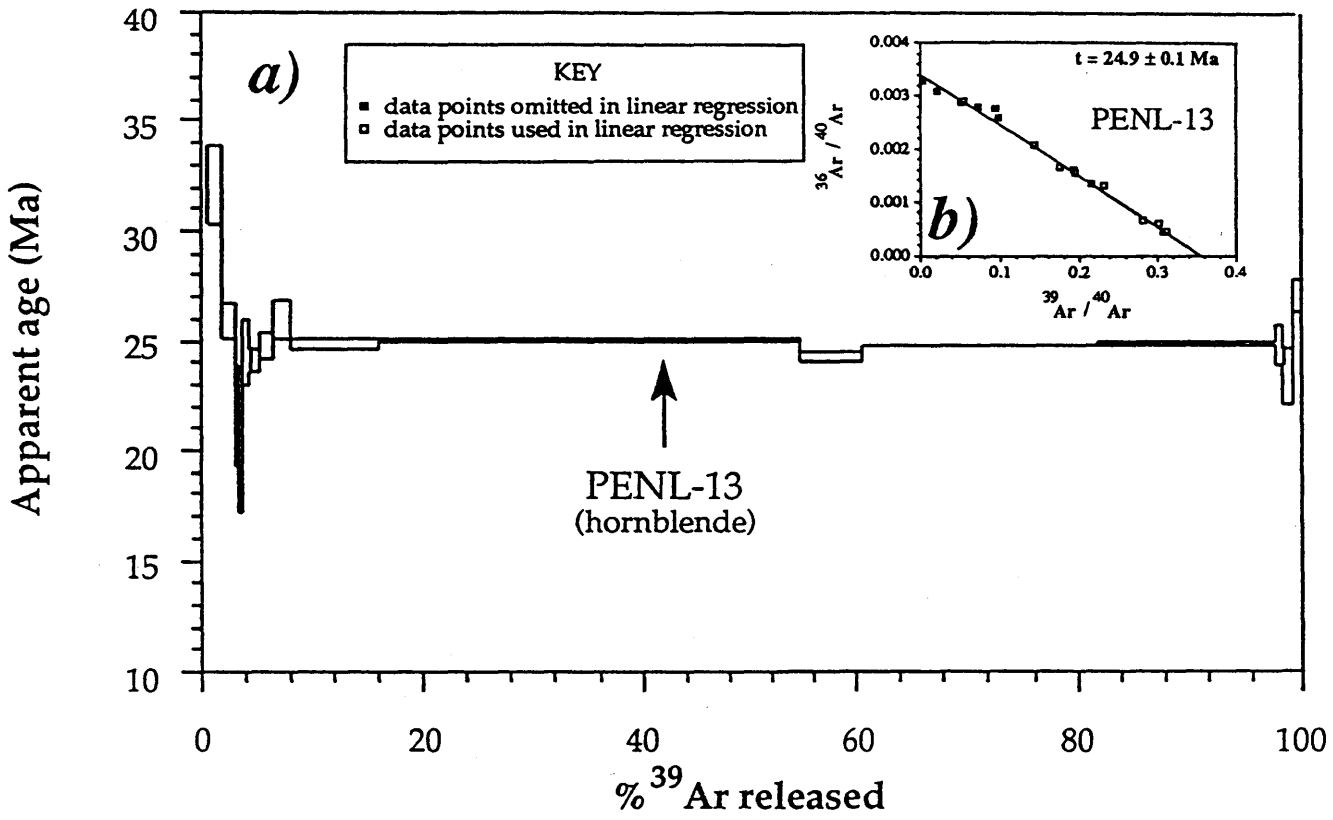
a)
KEY
data points omitted in linear regression
data points used in linear regression
b)
t = 24.9 ± 0.1 Ma
PENL-13
$^{36}Ar / ^{40}Ar$
$^{39}Ar / ^{40}Ar$
0.004
0.003
0.002
0.001
0.000
0.0
0.1
0.2
0.3
0.4
Apparent age (Ma)
40
35
30
25
20
15
10
PENL-13
(hornblende)
0
20
40
60
80
100
% ^{39}Ar released

Figure 7.

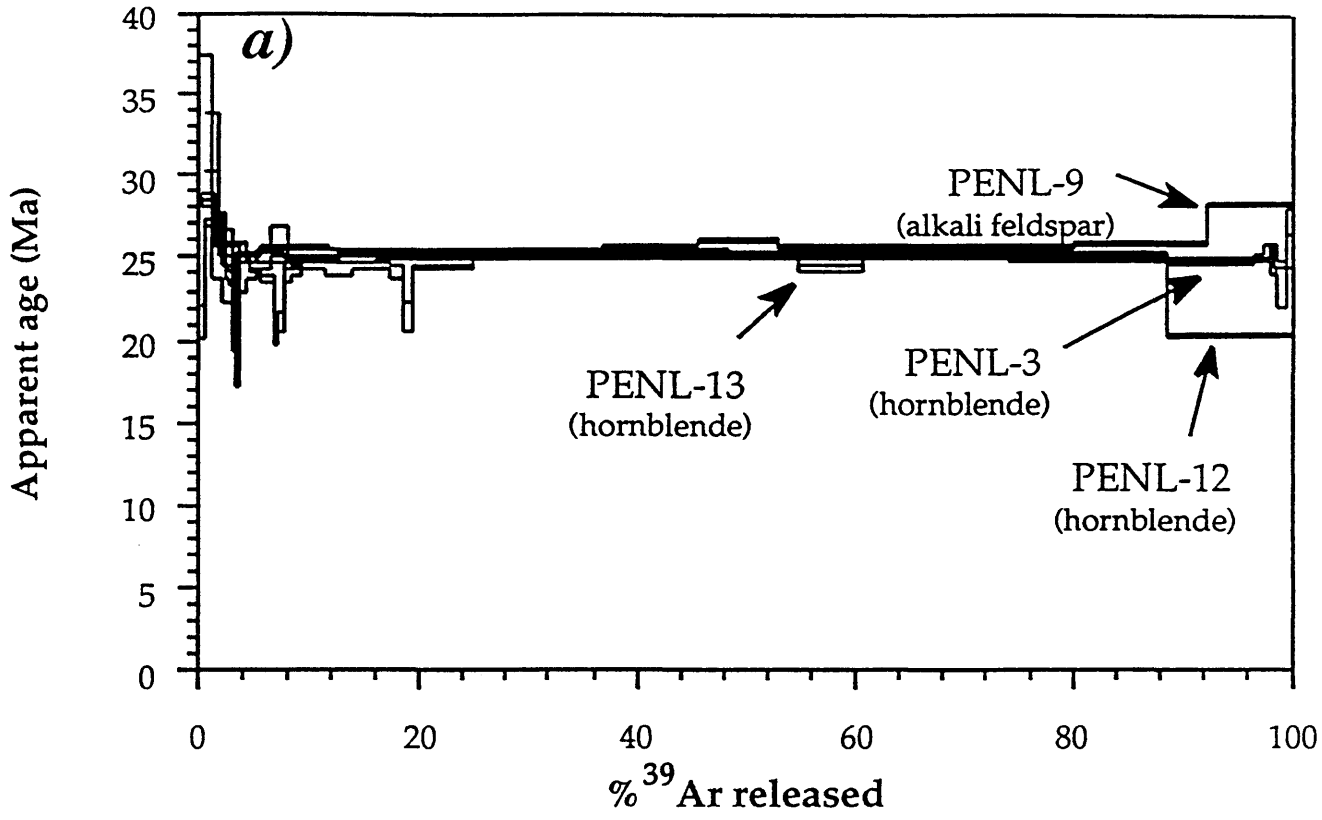

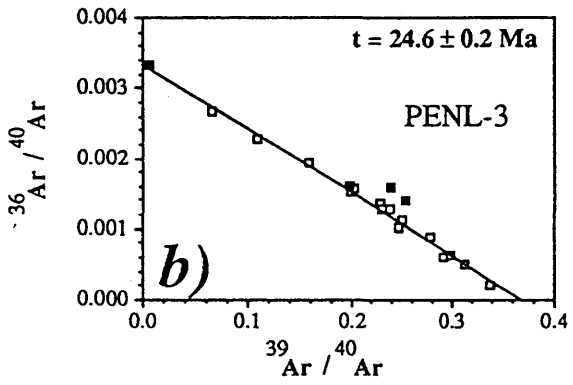

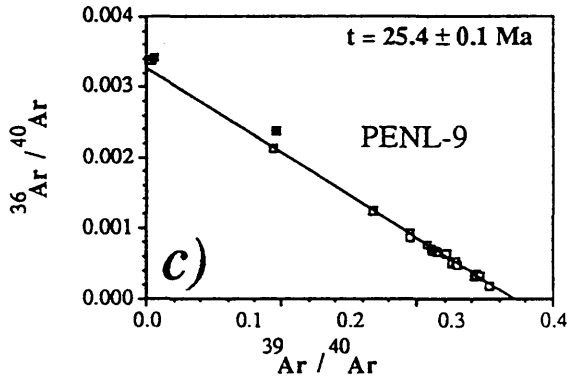

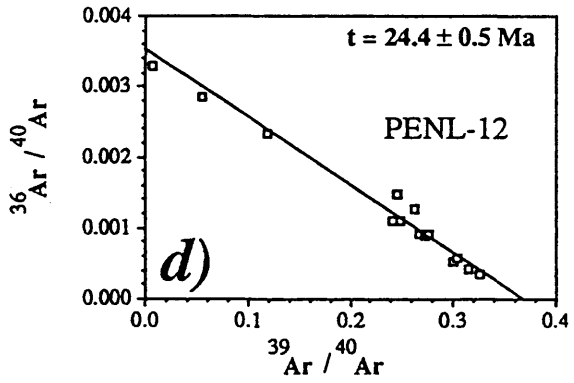

KEY
- data points omitted in linear regression
- data points used in linear regression

Figure 8.

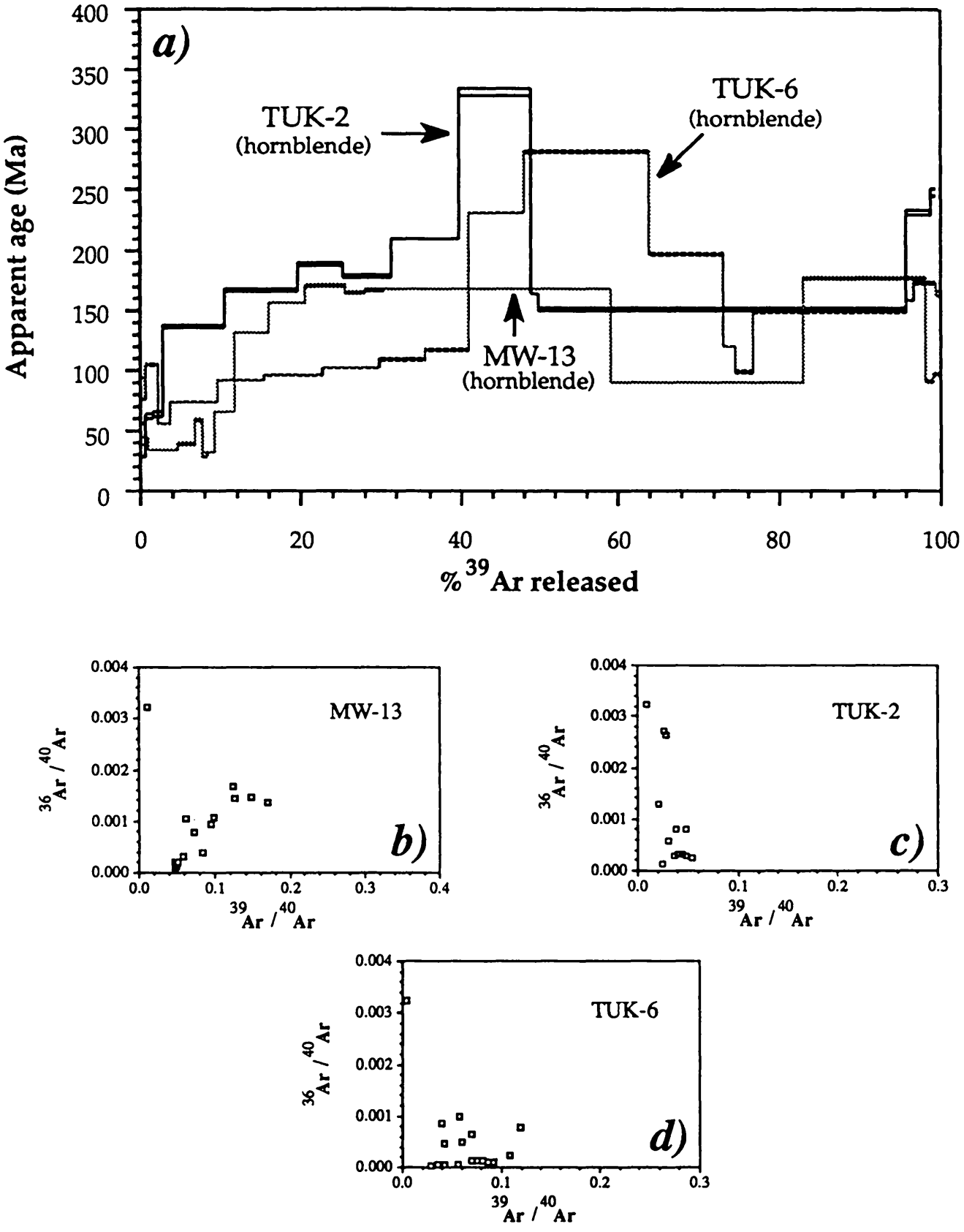
a)
TUK-2
(hornblende)
TUK-6
(hornblende)
MW-13
(hornblende)
Apparent age (Ma)
% 39Ar released
b)
MW-13
c)
TUK-2
d)
TUK-6
36Ar / 40Ar
39Ar / 40Ar

Figure 9.

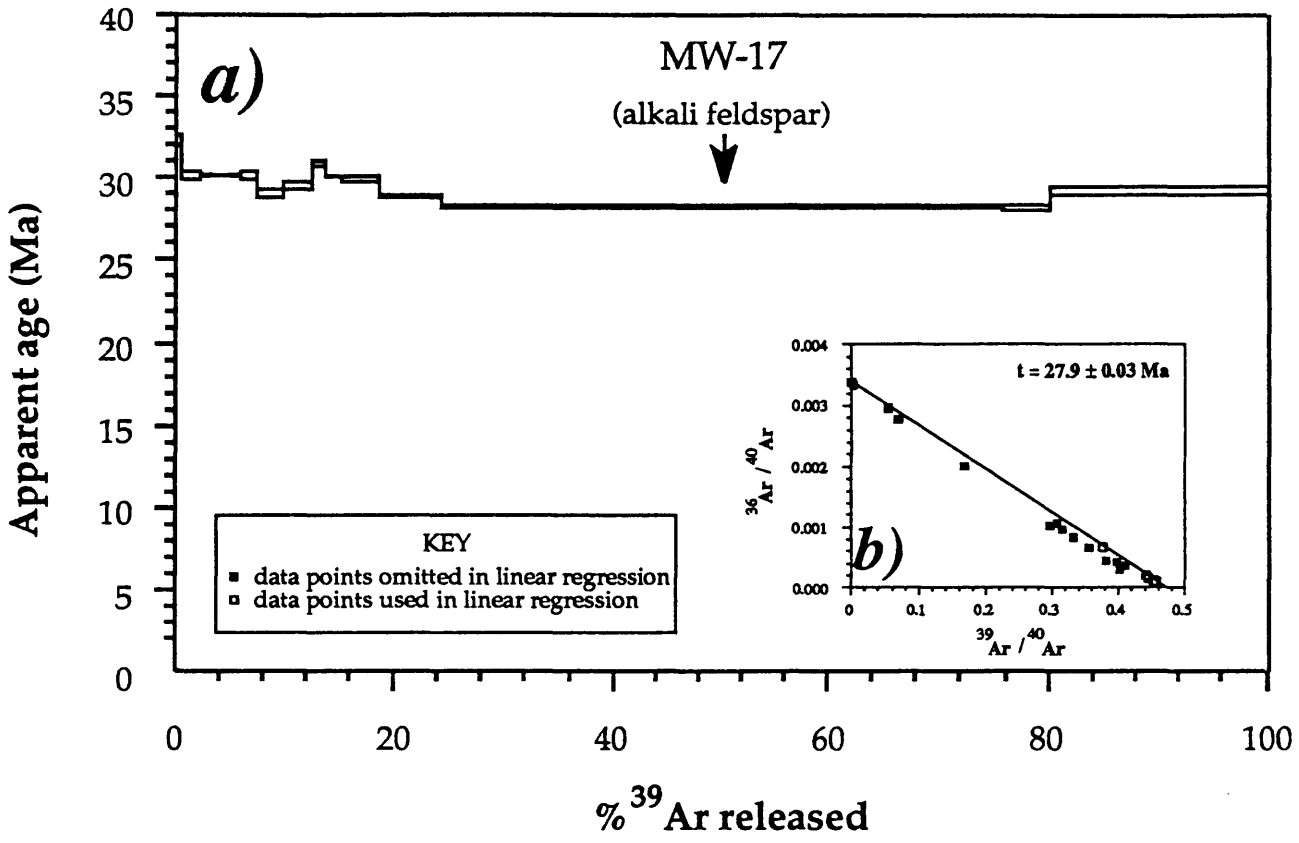
a)
MW-17
(alkali feldspar)
Apparent age (Ma)
40
35
30
25
20
15
10
5
0
0
20
40
60
80
100
% 39Ar released
KEY
data points omitted in linear regression
data points used in linear regression
b)
t = 27.9 ± 0.03 Ma
36Ar / 40Ar
39Ar / 40Ar
0.004
0.003
0.002
0.001
0.000
0
0.1
0.2
0.3
0.4
0.5

Figure 10.

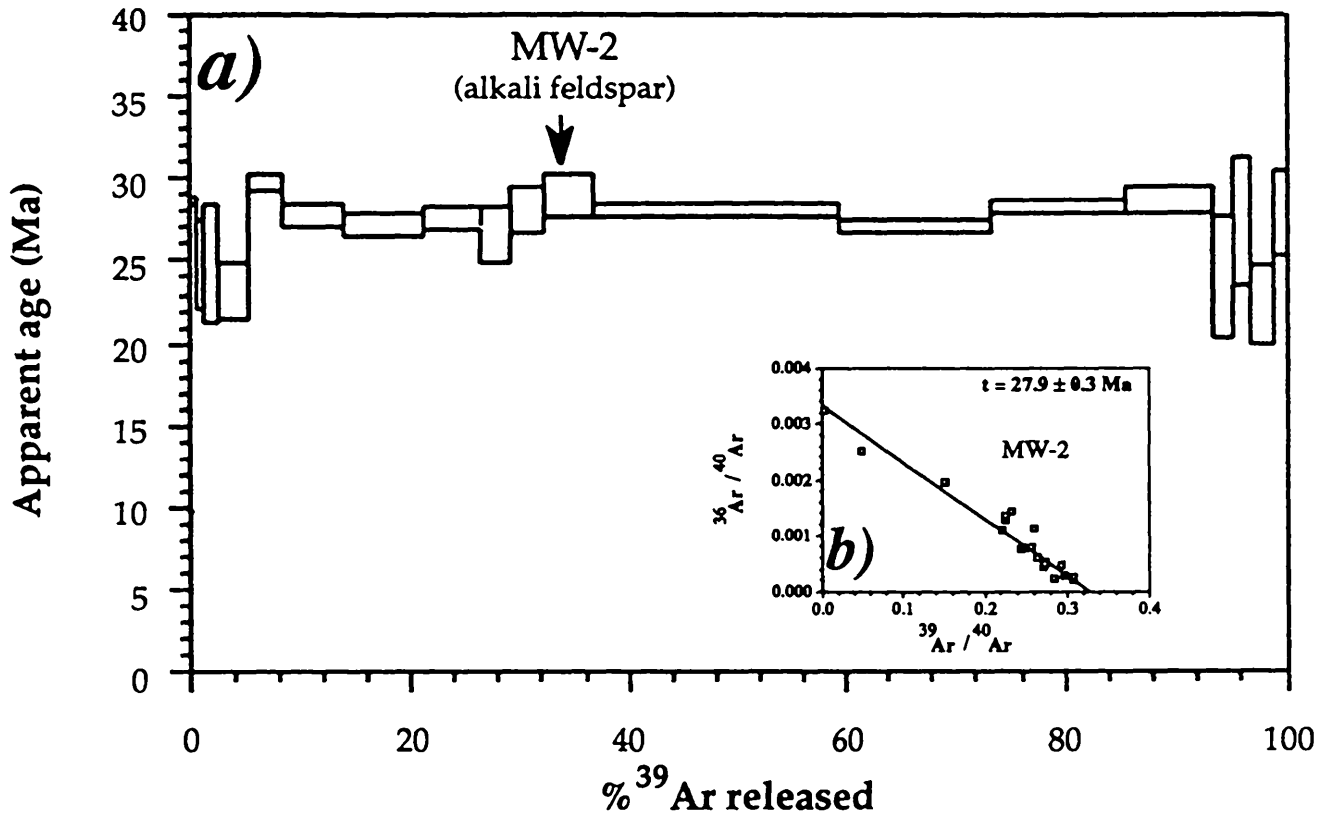
a)
MW-2
(alkali feldspar)
Apparent age (Ma)
0
5
10
15
20
25
30
35
40
0
20
40
60
80
100
% 39Ar released
b)
t = 27.9 ± 0.3 Ma
MW-2
36Ar / 40Ar
39Ar / 40Ar
0.000
0.001
0.002
0.003
0.004
0.0
0.1
0.2
0.3
0.4

Figure 11.

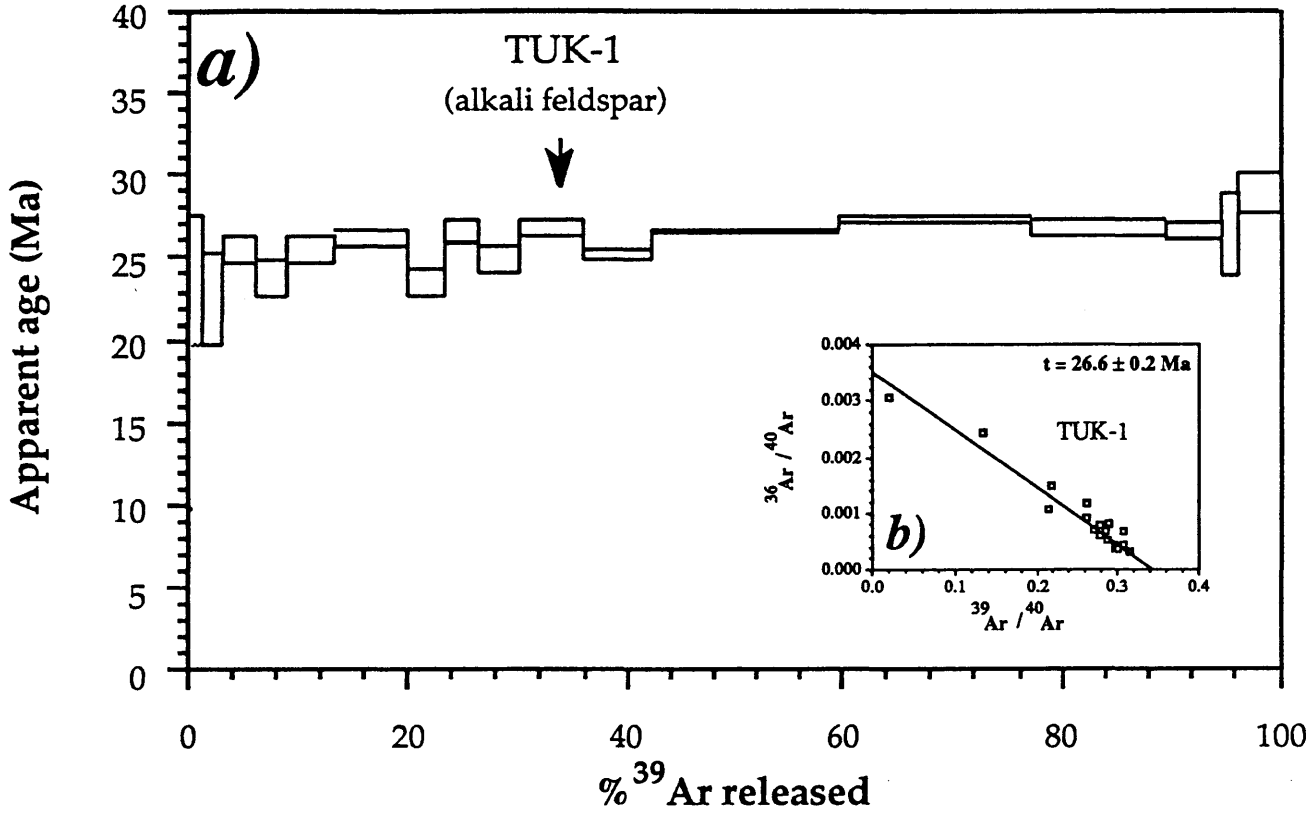
a)
TUK-1
(alkali feldspar)
Apparent age (Ma)
%39Ar released
b)
t = 26.6 ± 0.2 Ma
TUK-1
36Ar / 40Ar
39Ar / 40Ar

Figure 12.

Table 1. Previous age determinations of intrusive rocks from the Henry and La Sal Mountains, Utah. K-Ar ages calculated using decay constants reported by Steiger and Jager (1977).

SAMPLE	AGE (Ma)	ERROR (Ma)	METHOD	MATERIAL	LITHOLOGY	REFERENCE
HENRY MTNS.						
ELLN-1*	20	0.95	Fission-Track	zircon	Plagioclase-hornblende porphyry	1
PENL-1*	23.9	1.05	"	"	"	1
PENL-1*	26.4	1.25	"	sphene	"	1
HIL-1	29.2	1.15	"	zircon	"	1
HIL-2	21.2	1.2	"	"	"	1
HIL-2	25.6	1.65	"	sphene	"	1
BULL-1*	28.6	1.2	"	zircon	"	1
751 (Bull Mtn.)	44.8	NA	K-Ar	hornblende	"	2
Mt. Pennell	40.9	1.65	"	"	"	4
Mt. Ellen	40.8	2.25	"	"	"	4
Mt. Hillers	24.8	0.02	"	"	"	4
LA SAL MTNS.						
CSTV-2	28.7	1.35	Fission-Track	zircon	"	1
"	30.3	1.6	"	sphene	"	1
"	28.21	0.55	K-Ar	biotite	"	1
LAS-1	28.5	1.9	Fission-Track	sphene	syenite porphyry	1
749A	24.1	NA	K-Ar	hornblende + augite	Plagioclase-hornblende porphyry	2
LS-3-63	26.1	1.25	K-Ar	augite	syenite porphyry	3
LS-2-63	23.1	1.65	K-Ar	augite	"	3
LS-1-63	56.2	0.75	K-Ar	hornblende	Plagioclase-hornblende porphyry	3
"	494	0.1	$^{206}Pb/^{204}Pb$	zircon	"	3
"	756	0.4	$^{207}Pb/^{204}Pb$	zircon	"	3
"	794	0.25	$^{208}Pb/^{204}Pb$	zircon	"	3

*By coincidence, some sample prefixes used by Sullivan and others (1991) are the same as some used in this report.

REFERENCES:

1 Sullivan and others (1991).
2 Armstrong (1969).
3 Stern and other (1965).
4 Dubiel and others (1990).

Table 2. $^{40}Ar/^{39}Ar$ age determinations from the Henry and La Sal Mountains intrusions, Utah.

SAMPLE	N. LAT.	W. LONG.	$^{40}Ar/^{36}Ar$	$^{40}Ar^{*}/^{39}Ar_{K}$	J	MSWD	AGE (Ma)	±1 s.d.	MATERIAL ANALYZED	LITHOLOGY	INTRUSIVE CENTER	COMMENTS
BULL-1	38° 9' 6"	110° 44' 23"			0.0050261	n.d.	<31.9	0.4	hornblende	plagioclase-hornblende porphyry	Mt. Ellen	Inherited argon. Fission-track age of 28.6 ± 1.2 Ma* is considered best estimate of crystallization age.
ELLN-4	38° 4' 39"	110° 45' 21"			0.0050319	n.d.	<35.7	3.3	"	"	"	Inherited argon.
ELLN-10	38° 4' 29"	110° 45' 26"	320 ± 15	3.30863 ± 0.03171	0.0049700	173	29.4	0.3	"	"	"	
ELLN-7	38° 0' 10"	110° 47' 36"			0.0047909	n.d.	<28.4	0.5	"	"	Mt. Pennell	Inherited argon
"	"	"	302.3 ± 2.2	2.70879 ± 0.02869	0.0047909	0.75	23.3	0.2	"	"	"	Results from single crystal laser fusions. See text for discussion.
PENL-14	37° 57' 58"	110° 45' 33"	690 ± 51	2.61151 ± 0.23623	0.0048134	148	22.5	1.9	"	"	"	Age must be greater than about 25 Ma based on cross-cutting relationships. This is concordant within analytical error. See text for discussion.
PENL-13	37° 57' 0"	110° 46' 11"	293.1 ± 1.7	2.82955 ± 0.00656	0.0049043	7.5	24.9	0.1	"	"	"	
PENL-12	37° 57' 1"	110° 47' 50"	283 ± 12	2.72196 ± 0.05494	0.0050004	9.7	24.4	0.5	"	"	"	
PENL-9	37° 57' 13"	110° 47' 50"	305.5 ± 3.3	2.79397 ± 0.00445	0.0050738	10.8	25.4	0.1	alkali feldspar	syenite porphyry	"	
PENL-3	37° 56' 54"	110°46' 44"	300.4 ± 4.8	2.74228 ± 0.02704	0.0050156	36	24.6	0.2	hornblende	plagioclase-hornblende porphyry	"	
HILL-10KRS	37° 51' 26"	110° 42' 10"	464 ± 11	3.44632 ± 0.03944	0.00480005	0.64	29.6	0.4	"	"	Mt. Hillers	Two sets of data are reported because of two distinct trapped argon components in the sample. Interpreted age is 29.35 ± 0.33 Ma. See text for discussion.
"	"	"	316.8 ± 9.9	3.28337 ± 0.03468	0.0048005	7.3	29.1	0.3	"	"	"	
ELL-1KRS	37° 44' 50"	110° 37' 19"	310.8 ± 2.4	3.44058 ± 0.11118	0.0050770	6.97	31.2	1.0	"	"	Mt. Ellsworth	Homogeneous excess argon.
MW-13	38° 32' 34"	109° 14' 5"			0.0049390	n.d.	27.9-31.5	n.d.	"	"	North Mountain	Inherited argon. Age constrained by cross-cutting relationships with MW-2.
"	"	"					27.5	1.4	"	"	"	Results from single crystal laser fusions. Mean of three Oligocene ages. See text for discussion.
MW-2	38° 32' 19"	109° 14' 46"	302 ± 10	3.08077 ± 0.02991	0.0050530	2.3	27.9	0.3	alkali feldspar	syenite porphyry	"	
MW-17	38° 31' 19"	109° 13' 29"	296.7 ± 4.9	2.13906 ± 0.00122	0.007287	0.9	27.9	0.03	"	"	"	
TUK-1	38° 27' 23"	109° 15' 57"	285 ± 5.9	2.94181 ± 0.01607	0.0050676	3.7	26.7	0.2	"	"	Middle Mountain	
TUK-2	38° 28' 25"	109° 16' 5"			0.0048854	n.d.	<62.9	2.7	hornblende	plagioclase-hornblende porphyry	"	Inherited argon.
"	"	"					25.1	4.1	"	"	"	Results from single crystal laser fusions. Mean of nine Oligocene ages. See text for discussion.
TUK-6	38° 24' 51"	109° 15'45"			0.0049223	n.d.	<56.5	0.3	"	"	South Mountain	Inherited argon.
"	"	"					26.0	2.4	"	"	"	Results from single crystal laser fusions. Mean of two Oligocene ages. See text for discussion.

*Data from Sullivan and others (1991)

APPENDIX 1A

HENRY MOUNTAINS SAMPLES

BULL-1 HORNBLENDE (J=0.0050261)*

STEP	T °C	$^{40}Ar/^{39}Ar$[1]	$^{37}Ar/^{39}Ar$[1,2]	$^{36}Ar/^{39}Ar$[1] (e-3)	^{39}Ar (e-15 mol)	$\%^{39}Ar$ released	$^{40}Ar^{*}$[3] %	$^{40}Ar^{*}/^{39}Ar_K$	AGE ± 1s.d. Ma
1	700	701.2	1.732	23.36	0.773	0.499	1.55	10.92	96.4 ± 46.2
2	800	16.21	1.441	42.88	2.35	2.02	21.9	3.627	32.6 ± 0.6
3	850	11.26	1.385	26.35	1.49	2.98	29.6	3.551	31.9 ± 0.4
4	875	11.36	2.429	26.69	0.301	3.18	0.26	3.623	32.6 ± 2.3
5	925	11.59	3.682	24.04	0.775	3.68	37.1	4.727	42.4 ± 0.5
6	960	5.078	3.89	4.329	13.2	12.2	78.4	4.055	36.4 ± 0.1
7	980	4.525	3.767	3.339	9.45	18.3	81.4	3.785	34.0 ± 0.1
8	985	4.333	3.697	2.758	9.69	24.6	83.1	3.76	33.8 ± 0.2
9	990	4.276	3.69	2.388	6.85	29	83.9	3.811	34.2 ± 0.3
10	995	4.238	3.667	2.156	5.26	32.4	85	3.84	34.5 ± 0.1
11	1020	4.458	3.683	2.261	9.49	38.5	87.3	4.031	36.2 ± 0.2
12	1040	5.027	3.882	2.113	17.1	49.6	90.9	4.659	41.8 ± 0.2
13	1060	8.599	3.934	2.591	19.1	0.62	93.1	8.099	72.0 ± 0.2
14	1070	9.332	4.177	3.547	2.72	63.7	85.7	8.569	76.1 ± 0.3
15	1090	6.767	4.013	2.695	2.3	65.2	83.2	6.239	55.7 ± 0.2
16	1110	5.87	3.916	2.406	20.5	78.4	90.6	5.419	48.5 ± 0.0
17	1125	7.188	3.978	4.342	4.09	81.1	79.7	6.17	55.1 ± 0.2
18	1140	5.742	3.912	2.988	5.75	84.8	84.2	5.118	45.8 ± 0.2
19	1160	5.696	3.837	2.78	7.19	89.4	85.7	5.128	45.9 ± 0.2
20	1180	6.16	3.942	2.072	6.82	93.9	87.3	5.81	51.9 ± 0.1
21	1200	7.061	4.02	4.553	5.91	97.7	77.8	5.984	53.5 ± 0.4
22	1450	6.645	4.08	4.769	3.61	100	25.8	5.507	49.3 ± 0.2

ELLN-4 HORNBLENDE (J=0.0050319)

STEP	T °C	$^{40}Ar/^{39}Ar$	$^{37}Ar/^{39}Ar$	$^{36}Ar/^{39}Ar$ (e-3)	^{39}Ar (e-15 mol)	$\%^{39}Ar$ released	$^{40}Ar^{*}$ %	$^{40}Ar^{*}/^{39}Ar_K$	AGE ± 1s.d. Ma
1	700	42.58	0.6362	121.9	0.158	0.174	14.8	6.576	58.7 ± 12.1
2	800	23.84	1.138	67.42	0.616	0.856	16.3	3.975	35.7 ±3.3
3	900	30.15	2.841	83.47	0.775	0.172	18.4	5.667	50.7 ± 2.1
4	950	9.428	4.055	14.44	1.39	3.25	55.2	5.431	48.6 ± 1.0
5	975	6.256	4.498	7.471	1.39	4.79	64.7	4.347	39.0 ± 0.7
6	990	7.45	5.068	1.247	2.98	8.09	85.1	6.539	58.4 ± 0.3
7	1010	8.134	5.015	4.348	2.91	11.3	81.7	6.869	61.3 ± 0.5
8	1020	9.117	4.903	5.452	1.92	13.4	82.4	7.841	69.8 ±0.5
9	1030	8.167	5.264	3.687	61.9	0.82	90.2	7.438	66.3 ± 0.3
10	1040	6.761	4.641	5.626	0.635	82.8	67.4	5.409	48.4 ± 1.2
11	1070	7.962	4.463	9.143	1.06	83.9	63	5.559	49.8 ± 0.6
12	1090	7.526	5.168	3.572	5.63	90.2	88.4	6.822	60.9 ± 0.2
13	1130	8.031	5.269	3.825	5.33	96.1	87.8	7.261	64.7 ± 0.2
14	1200	8.645	5.301	6.19	3.31	99.7	78.6	1.178	64.0 ± 0.5
15	1450	21.06	4.889	0	0.233	100	27.9	22.13	190.5 ± 0.6

*J = value of the J-factor used for each sample.

[1]not corrected for interfering reactions. K correction ($^{40}Ar/^{39}Ar$) = 0.017; Ca correction ($^{36}Ar/^{37}Ar$) = 0.00023; Ca correction ($^{39}Ar/^{37}Ar$) = 0.000506.

[2]corrected for decay of ^{37}Ar.

[3]Includes blank.

ELLN-10 HORNBLENDE (J=0.0049700)

STEP	T °C	$^{40}Ar/^{39}Ar$	$^{37}Ar/^{39}Ar$	$^{36}Ar/^{39}Ar$ (e-3)	^{39}Ar (e-15 mol)	$\%^{39}Ar$ released	$^{40}Ar^*$ %	$^{40}Ar^*/^{39}Ar_K$	AGE ± 1s.d. Ma
1	700	282.8	0.7105	934.4	0.214	0.185	2.35	6.702	59.1 ± 18.1
2	800	93.59	1.698	287.6	0.378	0.512	9.13	8.712	76.5 ± 8.8
3	850	32.8	2.063	90.29	0.217	0.7	17.1	6.252	55.2 ± 6.4
4	900	18.31	2.353	48.83	0.222	0.892	17.96	4.031	35.8 ± 4.3
5	925	16.25	2.158	49.52	0.216	1.08	8.4	1.753	15.7 ± 2.3
6	970	8.975	4.758	19.38	1.86	2.69	36.9	3.562	31.7 ± 0.6
7	990	9.778	4.456	21.7	0.693	3.29	31.4	3.658	32.5 ± 0.6
8	1000	6.945	4.929	13.36	0.79	3.98	38.5	3.322	29.5 ± 0.7
9	1020	4.319	5.384	4.585	3.97	7.41	70.8	3.322	29.5 ± 0.3
10	1050	4.451	5.48	3.637	13	18.6	81.5	3.742	33.2 ± 0.4
11	1065	3.911	5.48	2.503	25.9	41.1	88.6	3.536	31.4 ± 0.1
12	1080	3.696	5.452	2.734	10.2	49.9	83.8	3.25	28.9 ± 0.1
13	1095	3.571	5.5	2.126	25	71.5	90.2	3.309	29.4 ± 0.1
14	1120	5.412	5.988	6.78	3.21	74.3	62.3	3.81	33.8 ± 0.3
15	1150	4.893	5.704	4.605	5.15	78.7	72.3	3.914	34.8 ± 0.2
16	1175	4.316	5.478	3.69	16.8	93.3	79.7	3.591	31.9 ± 0.1
17	1200	5.414	5.481	8.712	5.24	97.8	52.3	3.204	28.5 ± 0.4
18	1450	3.492	5.982	0.5423	2.55	100	12.1	3.732	33.2 ± 0.1

ELLN-7 HORNBLENDE (J=0.0047909)

STEP	T °C	$^{40}Ar/^{39}Ar$	$^{37}Ar/^{39}Ar$	$^{36}Ar/^{39}Ar$ (e-3)	^{39}Ar (e-15 mol)	$\%^{39}Ar$ released	$^{40}Ar^*$ %	$^{40}Ar^*/^{39}Ar_K$	AGE ± 1s.d. Ma
1	800	12.03	0.1932	27.85	4.03	3.47	31.2	3.799	32.5 ± 0.7
2	900	4.882	0.2422	5.327	2.73	5.82	0.64	3.308	28.4 ± 0.5
3	940	5.342	0.4492	6.633	1.67	7.26	56.6	3.397	29.1 ± 0.3
4	980	6.267	2.141	8.906	0.804	7.95	52.3	3.768	32.3 ± 0.5
5	1010	5.116	2.758	5.666	1.53	9.27	63.8	3.618	31.0 ± 0.5
6	1025	5.637	2.978	6.973	2.76	11.6	61.5	3.768	32.3 ± 0.5
7	1040	6.213	3.334	6.03	2.2	13.5	67.6	4.648	39.7 ± 0.4
8	1050	6.038	3.667	5.207	2.05	15.3	70.3	4.74	40.5 ± 0.4
9	1070	6.678	4.263	9.444	6.28	20.7	60.1	4.169	35.7 ± 0.2
10	1090	6.231	4.438	5.518	11.5	30.6	76.6	4.896	41.8 ± 0.2
11	1110	8.38	4.365	4.476	9.98	39.2	85.7	7.354	62.5 ± 0.4
12	1130	5.058	4.111	3.095	17.5	54.3	85.2	4.415	37.8 ± 0.2
13	1160	5.039	4.104	3.877	21.4	72.7	80.5	4.164	35.6 ± 0.2
14	1200	7.407	4.323	3.893	31.7	100	86.3	6.547	55.7 ± 0.1
SINGLE CRYSTAL LASER FUSIONS									
1	>1450	3.762	4.880	4.384	2.58		73.1	2.788	23.9 ± 0.6
2	"	10.53	2.892	26.49	2.04		27.3	2.883	25.7 ± 0.5
3	"	3.234	3.349	2.56	1.70		82.1	2.639	24.0 ± 0.6
4	"	3.891	2.419	4.426	3.30		69.9	2.734	24.4 ± 0.6

PENL-14 HORNBLENDE (J=0.0048134)

STEP	T°C	$^{40}Ar/^{39}Ar$	$^{37}Ar/^{39}Ar$	$^{36}Ar/^{39}Ar$ (e-3)	^{39}Ar (e-15 mol)	$\%^{39}Ar$ released	$^{40}Ar^*$ %	$^{40}Ar^*/^{39}Ar_K$	AGE ± 1s.d. Ma
1	800	61.41	0.6482	182.6	0.908	0.981	12.1	7.471	63.7 ± 3.9
2	900	14.95	0.8899	31.62	0.478	1.5	34.1	5.651	48.4 ± 2.7
3	970	11.26	3.44	21.16	1.1	2.69	41.5	5.229	44.8 ± 1.0
4	1000	5.979	4.086	5.695	1.63	4.45	63.9	4.566	39.2 ± 0.4
5	1020	4.06	4.487	3.05	6.46	11.4	78.5	3.455	29.8 ± 0.1
6	1040	3.963	4.599	2.783	8.54	20.7	81.4	3.444	29.7 ± 0.2
7	1050	4.352	4.625	3.342	5.46	26.6	76.6	3.67	31.6 ± 0.2
8	1065	4.674	4.615	3.251	3.63	30.5	74.8	4.019	34.6 ± 0.2
9	1085	4.642	4.549	3.356	4.91	35.8	76.4	3.952	34.0 ± 0.1
10	1100	5.215	4.558	3.836	3.18	39.2	74	4.385	37.7 ± 0.2
11	1140	5.519	4.946	3.931	9.41	49.4	79.9	4.688	40.3 ± 0.2
12	1150	7.51	4.992	8.34	5.49	55.3	65.9	5.381	46.1 ± 0.2
13	1160	6.445	4.963	6.716	11.9	68.2	70.5	4.792	41.1 ± 0.1
14	1180	8.3	4.795	7.841	3.56	72	66.4	6.307	53.9 ± 0.3
15	1200	6.683	4.86	6.376	3.38	75.7	63.5	5.125	44.0 ± 0.2
16	1250	6.584	4.849	6.92	9.27	85.7	67.6	4.864	41.7 ± 0.2
17	1500	13.21	4.952	28.19	13.2	100	33.1	5.209	44.7 ± 0.6

PENL-13 HORNBLENDE (J=0.0049043)

STEP	T°C	$^{40}Ar/^{39}Ar$	$^{37}Ar/^{39}Ar$	$^{36}Ar/^{39}Ar$ (e-3)	^{39}Ar (e-15 mol)	$\%^{39}Ar$ released	$^{40}Ar^*$ %	$^{40}Ar^*/^{39}Ar_K$	AGE ± 1s.d. Ma
1	700	253.9	1.358	834.9	1.02	0.634	2.83	7.214	62.7 ± 7.4
2	800	45.07	1.552	140.4	2	1.88	8.08	3.674	32.2 ± 1.8
3	850	19.83	1.707	57.44	1.6	2.87	14.6	2.963	26.0 ± 0.8
4	900	13.81	1.768	38.72	0.708	3.31	16.3	2.473	21.7 ± 2.3
5	915	10.53	0.1694	28.85	0.474	3.61	15.9	2.001	17.6 ± 0.3
6	950	7.068	2.175	14.94	0.953	4.2	33.9	2.787	24.5 ± 1.5
7	975	5.161	2.425	8.651	1.54	5.16	46.3	2.755	24.2 ± 0.5
8	1000	5.12	2.688	8.297	2.11	6.47	49.3	2.828	24.9 ± 0.6
9	1020	5.707	2.858	9.921	2.46	8	47	2.956	26.0 ± 0.9
10	1040	4.654	2.813	6.779	12.6	15.8	59.1	2.828	24.9 ± 0.2
11	1060	3.559	2.723	2.958	62.2	54.5	79.3	2.857	25.1 ± 0.1
12	1070	3.324	2.875	2.492	9.53	60.5	78.8	2.77	24.3 ± 0.2
13	1090	3.263	2.911	2.061	34.1	81.7	85.4	2.839	24.9 ± 0.0
14	1110	3.24	3.352	2.1	26.1	97.9	85.2	2.836	24.9 ± 0.1
15	1140	4.316	5.525	6.29	1.28	98.7	45.2	2.824	24.8 ± 0.9
16	1175	10.14	11.32	27.91	1.21	99.5	21	2.663	23.4 ± 1.3
17	1225	18.17	25.1	56.88	0.658	99.9	12	3.091	27.1 ± 0.8
18	1450	22.59	1.156	19.88	0.152	100	2.35	16.78	142.7 ± 3.3

PENL-12 HORNBLENDE (J=0.0050004)

STEP	T°C	$^{40}Ar/^{39}Ar$	$^{37}Ar/^{39}Ar$	$^{36}Ar/^{39}Ar$ (e-3)	^{39}Ar (e-15 mol)	$\%^{39}Ar$ released	$^{40}Ar^*$ %	$^{40}Ar^*/^{39}Ar_K$	AGE ± 1s.d. Ma
1	800	129.9	1.131	427.2	1.76	1.14	2.83	3.689	33.0 ± 4.5
2	900	18.54	1.493	53.3	1.65	2.21	15.3	2.874	25.7 ± 1.9
3	950	8.487	1.861	20.22	1.67	3.3	29.7	2.623	23.5 ± 1.0
4	980	4.157	2.461	5.107	6.37	7.44	65.8	2.802	25.1 ± 0.3
5	1000	3.752	2.513	3.927	5.59	11.1	70.9	2.749	24.6 ± 0.3
6	1010	3.697	2.552	3.892	4.25	13.8	70	2.707	24.3 ± 0.4
7	1020	3.525	2.634	3.237	4.68	16.9	71.2	2.734	24.5 ± 0.2
8	1030	3.648	2.595	3.753	2.1	18.2	67.2	2.702	24.2 ± 0.4
9	1040	3.82	2.572	5.318	1.36	19.1	54.7	2.409	21.6 ± 0.9
10	1055	4.048	2.67	5.023	8.67	24.8	65.8	2.732	24.5 ± 0.1
11	1070	3.647	2.597	2.356	37.8	49.3	83.4	2.814	25.2 ± 0.1
12	1085	3.203	2.671	1.957	37.9	74	86.4	2.793	25.0 ± 0.1
13	1100	3.094	2.64	1.61	16	84.4	88	2.785	24.9 ± 0.2
14	1120	3.319	2.967	2.465	6.49	88.6	79.4	2.779	24.9 ± 0.2
15	1200	4.077	0.7758	6.245	17.3	99.9	54.2	2.268	20.3 ± 0.1
16	1450	14.98	20.23	0	0.224	100	17.3	17.03	147.4 ± 0.5

PENL-9 ALKALI FELDSPAR (J=0.0050738)

STEP	T°C	$^{40}Ar/^{39}Ar$	$^{37}Ar/^{39}Ar$	$^{36}Ar/^{39}Ar$ (e-3)	^{39}Ar (e-15 mol)	$\%^{39}Ar$ released	$^{40}Ar^*$ %	$^{40}Ar^*/^{39}Ar_K$	AGE ± 1s.d. Ma
1	450	978.4	0.3226	3304	1.37	0.184	0.23	2.235	20.3 ± 205
2	500	354.3	0.1713	1194	1.04	0.323	0.41	1.468	13.4 ± 212
3	550	7.842	0.0509	18.56	1.78	0.561	29.3	2.343	21.3 ± 1.0
4	600	8.017	0.0347	16.98	5.47	1.29	36.9	2.984	27.1 ± 0.2
5	630	4.515	0.0036	5.579	16.8	3.55	62.8	2.85	25.9 ± 0.1
6	650	3.415	0.0358	2.126	15.1	5.57	80.6	2.772	25.2 ± 0.1
7	680	3.545	0.0034	2.363	18.8	8.1	79.3	2.83	25.7 ± 0.1
8	720	3.59	0.0354	2.516	25.8	11.6	78.4	2.832	25.7 ± 0.1
9	780	3.132	0.0395	1.013	24.5	14.9	89.2	2.818	25.6 ± 0.0
10	800	3.113	0.0445	1.024	22.5	17.9	88.7	2.797	25.4 ± 0.1
11	820	3.31	0.053	1.664	0.19	20.4	83.8	2.805	25.5 ± 0.1
12	860	3.068	0.0582	0.9326	21.8	23.3	89.5	2.78	25.3 ± 0.1
13	900	3	0.0566	0.5954	24.6	26.6	92.4	2.811	25.6 ± 0.0
14	950	3.11	0.0514	1.008	22.8	29.7	88.6	2.798	25.4 ± 0.0
15	1000	3.309	0.0468	1.744	20.1	32.4	82.4	2.78	25.3 ± 0.1
16	1050	3.64	.0.419	2.782	31.1	36.6	75.9	2.804	25.5 ± 0.1
17	1100	3.872	0.0349	3.503	65.4	45.3	72	2.823	25.7 ± 0.0
18	1125	3.861	0.0344	3.29	56.1	52.9	73.3	2.875	26.1 ± 0.1
19	1150	3.531	0.0379	2.332	94.9	65.6	78.2	2.827	25.7 ± 0.1
20	1175	3.286	0.0345	1.554	1.08	80	83.4	2.812	25.6 ± 0.1
21	1200	3.361	0.0253	1.701	50.7	86.8	83	2.843	25.8 ± 0.1
22	1250	3.564	0.0356	2.399	39.1	92.1	76.7	2.84	25.8 ± 0.1
23	1550	3.14	0.0209	0.0203	59.1	100	25.9	3.118	28.3 ± 0.1

PENL-3 HORNBLENDE (J=0.0050158)

STEP	T°C	$^{40}Ar/^{39}Ar$	$^{37}Ar/^{39}Ar$	$^{36}Ar/^{39}Ar$ (e-3)	^{39}Ar (e-15 mol)	$\%^{39}Ar$ released	$^{40}Ar^*$ %	$^{40}Ar^*/^{39}Ar_K$	AGE ± 1s.d. Ma
1	700	131.4	0.5477	431.3	1.16	0.394	3	3.949	35.4 ± 6.7
2	800	15.25	0.4622	40.91	3.01	1.42	20.5	3.18	28.5 ± 0.4
3	850	9.162	0.478	20.96	2.57	2.29	31.5	2.985	26.8 ± 0.9
4	875	6.29	0.4515	12.27	1.58	2.83	38.7	2.679	24.1 ± 0.3
5	925	4.964	0.7339	7.878	2.69	3.74	49.8	2.652	23.8 ± 0.4
6	950	5.042	0.8074	7.756	2.5	4.59	50.8	2.789	25.1 ± 0.3
7	975	4.359	1.183	5.829	2.82	5.55	56.4	2.702	24.3 ± 0.1
8	985	4.235	1.396	5.686	2.82	6.51	56.3	2.635	23.7 ± 0.2
9	990	4.182	1.235	6.755	1.23	6.93	42.9	2.254	20.3 ± 0.4
10	1000	3.959	1.514	5.709	1.48	7.43	48.5	2.359	21.2 ± 0.6
11	1010	4.005	1.731	4.794	2.13	8.15	57.9	2.692	24.2 ± 0.6
12	1020	3.61	2.015	3.486	2.39	8.97	64.2	2.703	24.3 ± 0.3
13	1050	3.362	2.62	2.595	9.89	12.3	78.2	2.759	24.8 ± 0.1
14	1075	4.064	2.916	4.767	14.8	17.4	67.8	2.841	25.5 ± 0.1
15	1100	3.466	3	2.78	90.8	48.2	80.9	2.835	25.5 ± 0.1
16	1125	2.968	3.05	1.248	118	88.5	92.1	2.794	25.1 ± 0.2
17	1150	3.207	3.414	2.257	24.1	96.6	83.1	2.76	24.8 ± 0.2
18	1175	4.328	5.22	6.605	2.2	97.4	48.3	2.775	24.9 ± 0.2
19	1200	5.047	6.221	8.971	2.68	98.3	43.8	2.81	25.3 ± 0.4
20	1450	1.092	9.909	0	4.99	100	12.6	2.709	24.3 ± 0.0

HILL-10KRS HORNBLENDE (J=0.0048005)

STEP	T°C	$^{40}Ar/^{39}Ar$	$^{37}Ar/^{39}Ar$	$^{36}Ar/^{39}Ar$ (e-3)	^{39}Ar (e-15 mol)	$\%^{39}Ar$ released	$^{40}Ar^*$ %	$^{40}Ar^*/^{39}Ar_K$	AGE ± 1s.d. Ma
1	800	46.83	1.822	140.6	0.37	0.45	11.1	5.396	46.1 ± 5.7
2	900	24.67	2.736	66.39	0.349	0.874	19.4	5.225	44.7 ± 4.8
3	970	7.783	3.721	13.01	0.833	1.89	46.5	4.183	35.9 ± 1.3
4	990	4.838	4.175	5.141	1.96	4.27	67	3.594	30.9 ± 0.3
5	1000	4.244	4.261	3.582	2.43	7.23	13.6	2.465	29.8 ± 0.2
6	1015	4.017	4.328	2.765	3.77	11.8	80.4	3.485	29.9 ± 0.3
7	1030	4.075	4.383	2.812	6.22	19.4	82.4	3.533	30.3 ± 0.2
8	1040	4.239	4.414	2.997	5.24	25.7	81	3.645	31.3 ± 0.2
9	1050	4.527	4.455	3.196	4.6	31.3	80.4	3.877	33.3 ± 0.4
10	1060	4.945	4.432	3.994	4.38	36.6	76.8	4.058	34.8 ± 0.2
11	1070	5.641	4.438	5.461	2.83	40.1	69.7	4.322	37.0 ± 0.3
12	1085	6.312	4.42	6.971	2.53	43.2	65.1	4.546	38.9 ± 0.3
13	1100	7.688	4.322	11.09	1.41	44.9	52.4	4.697	40.2 ± 0.5
14	1120	9.932	4.362	18.48	2.64	48.1	44.6	4.763	40.8 ± 0.4
15	1160	5.658	4.544	5.336	18	70	75.3	4.383	37.6 ± 0.2
16	1200	7.762	4.558	6.862	19.3	93.5	75.9	6.041	51.6 ± 0.3
17	1450	71.42	4.578	217.7	5.33	100	9.46	7.394	62.9 ± 4.2

ELL-1KRS HORNBLENDE (J=0.005077)

STEP	T °C	$^{40}Ar/^{39}Ar$	$^{37}Ar/^{39}Ar$	$^{36}Ar/^{39}Ar$ (e-3)	^{39}Ar (e-15 mol)	$\%^{39}Ar$ released	$^{40}Ar^*$ %	$^{40}Ar^*/^{39}Ar_K$	AGE ± 1s.d. Ma
1	450	748.5	1.291	2431	0.146	0.094	4.02	30.18	257.2±77.9
2	800	20.33	0.5599	53.17	0.701	0.546	22.1	4.636	42.0 ± 3.8
3	900	16.38	1.22	43.55	0.383	0.793	20.4	3.577	32.5 ± 3.4
4	970	24.21	2.339	65.65	0.46	1.09	19.3	4.957	44.8 ±7.8
5	1000	28.96	3.527	84.79	0.958	1.71	13.9	4.137	37.5 ± 2.8
6	1015	37.89	3.823	109.7	1.02	2.36	14.8	5.743	51.8 ± 4.4
7	1025	31.65	3.922	92.67	0.964	2.99	13.9	4.526	41.0 ± 2.4
8	1030	26.02	3.954	74.02	2.39	4.52	16.7	4.405	39.9 ± 2.2
9	1040	21.68	3.631	60.44	2.25	5.97	18.4	4.072	36.9 ± 1.5
10	1050	18.13	4.032	48.15	3.41	8.17	22.6	4.165	37.8 ± 1.9
11	1060	16.34	4.066	43.15	5.19	11.5	23.3	3.859	35.0 ± 0.6
12	1070	17.56	4.075	46.95	5.05	14.8	22.2	3.956	35.9 ± 0.6
13	1080	20.42	4.075	55.42	5.65	18.4	20.9	4.309	39.0 ± 0.5
14	1095	29.12	4.136	81.91	5.11	21.7	17.7	5.189	46.9 ± 1.2
15	1110	26.11	4.165	72.89	5.9	25.5	18.4	4.843	43.8 ± 1.5
16	1130	16.7	4.195	43.28	14	34.6	24.8	4.187	37.9 ± 0.4
17	1160	8.037	4.262	15.67	18.8	46.7	45.4	3.688	33.5 ± 0.4
18	1200	11.37	4.223	21.89	24.5	62.5	45.1	5.185	46.9 ± 0.2
19	1450	106.6	4.262	332.1	58.2	100	7.59	8.746	78.4 ± 5.7

LA SAL MOUNTAINS SAMPLES

MW-13 HORNBLENDE (J=0.004939)

STEP	T °C	$^{40}Ar/^{39}Ar$	$^{37}Ar/^{39}Ar$	$^{36}Ar/^{39}Ar$ (e-3)	^{39}Ar (e-15 mol)	$\%^{39}Ar$ released	$^{40}Ar^*$ %	$^{40}Ar^*/^{39}Ar_K$	AGE ± 1s.d. Ma
1	700	96.54	0.1232	310.5	1.49	0.978	4.94	4.782	42.1 ± 3.6
2	800	8.09	0.1838	13.56	5.21	4.39	50	4.078	36.0 ± 0.3
3	850	7.917	0.2805	11.47	3.51	6.69	56.4	4.53	39.9 ± 0.5
4	860	10.11	0.6323	10.9	1.43	7.63	66.5	6.913	60.6 ± 0.9
5	880	5.933	0.521	8.076	0.903	8.22	55.5	3.566	31.5 ± 1.4
6	910	6.741	1.149	10.14	1.34	9.09	53.6	3.809	33.6 ± 0.5
7	950	10.61	2.44	10.42	3.75	11.6	71.4	7.685	67.2 ± 0.5
8	990	17.01	2.741	6.027	6.49	15.8	90	15.42	132.4 ± 0.5
9	1010	19.44	2.978	4.583	7.16	20.5	93.5	18.3	156.1 ± 0.5
10	1020	21.34	3.092	4.583	7.2	25.2	94.1	20.21	171.6 ± 0.3
11	1030	20.49	3.098	4.365	3.74	27.6	93.7	19.42	165.3 ± 0.5
12	1040	21.05	3.086	5.221	3.88	30.2	92.7	19.73	167.8 ± 0.8
13	1070	20.52	3.545	3.498	44	59	95.6	19.74	167.9 ± 0.2
14	1090	11.81	3.072	5.199	36.6	82.9	87.1	10.48	91.0 ± 0.5
15	1120	21.42	3.707	2.781	23.3	98.2	96.1	20.87	177.0 ± 0.7
16	1160	13.7	5.684	11.9	1.66	99.3	72.6	10.58	91.9 ± 1.1
17	1200	16.11	6.806	17.92	1.12	100	63.5	11.3	98.0 ± 1.0
SINGLE CRYSTAL LASER FUSIONS (J=0.007278)									
1	>1450	3.044	2.688	3.384	5.37		72.1	2.201	28.7±0.6
2	"	7.751	2.568	4.911	5.06		83.1	6.453	82.8±0.7
3	"	2.861	2.907	3.392	3.49		70.7	2.03	26.5±1.1
4	"	3.398	3.584	5.152	5.61		61.4	2.093	27.3±0.7
5	"	4.04	2.940	3.858	4.77		75.9	3.076	39.9±0.7

MW-2 ALKALI FELDSPAR (J=0.005053)

STEP	T °C	$^{40}Ar/^{39}Ar$	$^{37}Ar/^{39}Ar$	$^{36}Ar/^{39}Ar$ (e-3)	^{39}Ar (e-15 mol)	$\%^{39}Ar$ released	$^{40}Ar^*$ %	$^{40}Ar^*/^{39}Ar_K$	AGE ± 1s.d. Ma
1	450	651.1	0.094	2113	0.15	0.202	4.09	26.64	227.9 ± 191
2	500	20.3	0.0703	51.01	0.154	0.41	24.9	5.214	46.9 ± 18.0
3	550	6.579	0.0234	12.92	0.463	1.04	40.4	2.747	24.9 ± 2.6
4	600	4.483	0.0276	5.765	0.948	2.32	60.2	2.764	25.0 ± 3.6
5	650	3.862	0.0348	4.32	1.98	4.99	65.7	2.571	23.3 ± 1.6
6	700	3.556	0.0337	0.8293	2.31	8.11	91.6	3.296	29.8 ± 0.5
7	750	3.399	0.0379	1.008	4.23	13.8	90.2	3.087	27.9 ± 0.7
8	800	3.275	0.04	0.8573	5.24	20.9	91.3	3.008	27.2 ± 0.7
9	850	3.28	0.0397	0.694	3.88	26.1	92.6	3.06	27.7 ± 0.7
10	900	3.442	0.0358	1.655	2.16	29.1	84.2	2.938	26.6 ± 1.7
11	950	3.687	0.0309	1.918	2.12	31.9	93.2	3.105	28.1 ± 1.4
12	1000	3.718	0.0268	1.623	3.44	36.6	86	3.223	29.1 ± 1.3
13	1050	3.686	0.027	1.873	6.34	45.1	84.2	3.117	28.2 ± 0.4
14	1100	3.819	0.0305	2.33	10.4	59.3	81.4	3.116	28.2 ± 0.4
15	1130	3.927	0.0357	3.076	10.3	73.1	76.3	3.004	27.2 ± 0.4
16	1150	4.07	0.0409	3.139	9.2	85.6	76.7	3.128	28.3 ± 0.4
17	1170	4.129	0.0436	3.172	5.88	93.5	76.7	3.117	28.7 ± 0.8
18	1200	4.456	0.0499	6.03	1.28	95.2	58.7	2.661	24.1 ± 3.6
19	1250	4.528	0.0443	5.002	1.19	96.8	65.8	3.036	27.5 ± 3.9
20	1300	4.325	0.0516	6.21	1.46	98.8	56.4	2.477	22.4 ± 2.4
21	1550	6.039	0.1551	9.973	0.876	100	50.1	3.086	27.9 ± 2.6

MW-17 ALKALI FELDSPAR (J=0.007287)

STEP	T °C	$^{40}Ar/^{39}Ar$	$^{37}Ar/^{39}Ar$	$^{36}Ar/^{39}Ar$ (e-3)	^{39}Ar (e-15 mol)	$\%^{39}Ar$ released	$^{40}Ar^*$ %	$^{40}Ar^*/^{39}Ar_K$	AGE ± 1s.d. Ma
1	450	4848	0.4018	16317	0.278	0.043	0.55	26.68	320.5±1502
2	500	317.7	0.6527	1066	0.728	0.156	0.84	2.680	34.9±55.8
3	550	18.0	0.0490	53.01	0.973	0.306	12.4	2.313	30.2±3.8
4	600	14.33	0.0708	39.48	2.08	0.628	18.0	2.648	34.5±2.7
5	650	5.985	0.0369	11.90	3.86	1.23	39.6	2.447	31.9±0.5
6	700	3.042	0.0155	2.471	10.1	2.79	73.4	2.289	29.8±0.2
7	750	2.642	0.0016	1.137	24.9	6.65	85.4	2.282	29.8±0.1
8	800	2.521	0.0162	0.7309	7.07	7.75	86.8	2.282	29.8±0,2
9	850	2.540	0.0143	1.039	16.5	10.3	85.4	2.210	28.8±0.2
10	900	3.283	0.0144	3.463	16.1	12.8	67.1	2.236	29.2±0.2
11	950	3.392	0.0167	3.448	7.61	14.0	67.2	2,350	30.6±0.1
12	1000	3.198	0.0225	3.006	11.1	15.7	69.8	2.287	29.8±0.1
13	1050	2.836	0.0229	1.849	20.5	18.9	77.6	2.267	29.6±0.2
14	1080	2.471	0.0117	0.8655	37.0	24.6	86.5	2.192	28.6±0.1
15	1110	2.276	0.0119	0.3507	102	40.4	92.7	2.149	28.0±0.1
16	1140	2.231	0.0115	0.2388	112	57.7	93.8	2.138	27.9±0.1
17	1170	2.217	0.0115	0.1866	73.9	69.1	94.2	2.138	27.9±0.1
18	1200	2.688	0.0135	1.772	44.2	76.0	76.4	2.141	27.9±0.1
19	1230	2.288	0.0186	0.4545	27.8	80.3	86.3	2.131	27.8±0.2
20	1550	2.177	0.0208	0.0	127	100	50.7	2.221	29.0±0.2

TUK-1 ALKALI FELDSPAR (J=0.0050676)

STEP	T °C	$^{40}Ar/^{39}Ar$	$^{37}Ar/^{39}Ar$	$^{36}Ar/^{39}Ar$ (e-3)	^{39}Ar (e-15 mol)	$\%^{39}Ar$ released	$^{40}Ar^*$ %	$^{40}Ar^*/^{39}Ar_K$	AGE ± 1s.d. Ma
1	450	52.12	0.0588	172.3	0.684	0.635	2.28	1.193	10.9 ± 5.4
2	500	7.471	0.0383	18.08	0.312	0.924	27.1	2.114	19.2 ± 9.3
3	550	4.615	0.0223	6.816	0.943	1.8	54.8	2.585	23.5 ± 3.6
4	600	3.834	0.0321	4.512	1.85	3.51	63.9	2.486	22.6 ± 2.8
5	650	3.582	0.0322	2.384	3.4	6.67	79	2.809	25.5 ± 0.8
6	700	3.487	0.0318	2.842	2.85	9.32	74.7	2.632	23.9 ± 1.0
7	750	3.282	0.038	1.497	4.65	13.6	85.5	2.825	25.6 ± 0.8
8	800	3.206	0.0375	0.9849	7.06	20.2	90.1	2.901	26.3 ± 0.5
9	850	3.271	0.0442	2.22	3.78	23.7	78.9	2.601	23.6 ± 0.7
10	900	3.407	0.0441	1.554	3.19	26.7	85.3	2.934	26.6 ± 0.7
11	950	3.617	0.0509	2.877	3.95	30.3	75.6	2.753	25.0 ± 0.8
12	1000	3.608	0.0476	2.139	6.21	36.1	81.7	2.962	26.9 ± 0.5
13	1050	3.857	0.0358	3.558	6.72	42.3	72.1	2.791	25.3 ± 0.3
14	1100	3.503	0.0295	1.874	18.8	59.8	83.6	2.934	26.6 ± 0.1
15	1125	3.398	0.0304	1.283	18.6	77.0	88.3	3.004	27.3 ± 0.2
16	1150	3.348	0.0321	1.251	13.5	89.6	88.3	2.963	26.9 ± 0.5
17	1180	3.402	0.0352	1.542	5.58	94.7	85.7	2.932	26.6 ± 0.5
18	1230	3.715	0.0466	2.639	1.44	96.1	77.2	2.921	26.5 ± 2.5
19	1550	4.688	0.0539	5.044	4.22	100	67.6	3.184	28.9 ± 1.2

TUK-2 HORNBLENDE (J=0.0048854)

STEP	T °C	$^{40}Ar/^{39}Ar$	$^{37}Ar/^{39}Ar$	$^{36}Ar/^{39}Ar$ (e-3)	^{39}Ar (e-15 mol)	$\%^{39}Ar$ released	$^{40}Ar^*$ %	$^{40}Ar^*/^{39}Ar_K$	AGE ± 1s.d. Ma
1	700	129.1	0.4663	420	0.805	0.591	3.86	5.0	43.5 ± 14.1
2	800	34.03	1.756	90.96	1.21	1.48	21	7.258	62.9 ± 2.7
3	900	38.77	7.969	107.5	1.67	2.7	19.1	7.553	65.4 ± 2.6
4	975	21.25	4.759	17.98	10.3	10.3	76	16.28	138.0 ± 1.0
5	1000	21.87	4.256	1.58	12.4	19.4	90.4	19.95	167.8 ± 0.5
6	1010	25.02	4.186	8.958	7.75	25.1	89.8	22.68	189.6 ± 0.7
7	1020	23.64	4.177	8.748	8.38	31.2	89.5	21.36	179.1 ± 0.4
8	1030	27.5	4.176	8.806	11.5	39.7	90.9	25.22	209.6 ± 0.4
9	1040	43.21	4.243	7.714	12.3	48.7	94.5	41.30	331.5 ± 2.9
10	1050	25.43	4.388	20.99	1.51	49.8	73.5	19.55	164.6 ± 0.8
11	1100	19.29	4.433	5.791	62.9	96	91.2	17.9	151.3 ± 0.3
12	1150	33.87	4.856	20.84	3.94	98.9	81.2	28.09	232.0 ± 1.1
13	1200	49.33	5.722	65.79	1.08	99.6	57.4	30.35	249.5 ± 2.6
14	1450	275	6.121	0	0.488	100	91.2	276.6	1542±10.0
SINGLE CRYSTAL LASER FUSIONS (J=0.007331)									
1	>1450	2.912	4.584	5.023	1.2		58.3	1.714	22.5±3.8
2	"	2.535	4.571	1.745	1.11		90.4	3.319	30.4±3.1
3	"	7.046	4.837	11.56	3.35		55.7	3.939	51.4±1.0
4	"	5.451	4.312	13.49	3.56		31.7	1.732	22.8±1.0
5	"	5.006	3.811	10.37	3.32		43.3	2.175	28.5±1.3
6	"	2.688	4.826	5.835	1.07		46.5	1.266	16.7±3.8
7	"	8.005	3.754	20.94	1.53		25.5	2.047	26.9±2.4
8	"	2.457	4.834	3.585	1.82		68.9	1.719	22.6±1.8
9	"	3.083	4.694	5.059	2.80		60.7	1.883	24.7±1.1
10	"	16.89	4.903	34.97	1.67		40.6	6.877	88.7±3.3
11	"	4.872	5.257	7.614	1.68		60.4	2.958	38.7±1.6
12	"	3.003	4.721	5.410	2.71		56.3	1.7	22.3±1.2
13	"	2.556	4.756	3.093	1.73		75.3	1.941	25.5±1.9

TUK-6 HORNBLENDE (J=0.0049223)

STEP	T °C	$^{40}Ar/^{39}Ar$	$^{37}Ar/^{39}Ar$	$^{36}Ar/^{39}Ar$ (e-3)	^{39}Ar (e-15 mol)	$\%^{39}Ar$ released	$^{40}Ar^*$ %	$^{40}Ar^*/^{39}Ar_K$	AGE ± 1s.d. Ma
1	700	238.3	0.2165	772.9	0.793	0.574	4.15	9.94	86.2 ± 9.0
2	800	17.33	0.3264	17.07	1.91	1.96	69.5	12.29	106.0 ± 0.9
3	900	8.426	0.6088	6.733	2.27	3.61	73.2	6.463	56.5 ± 0.3
4	950	9.294	2.89	2.773	8.12	9.49	91.8	8.667	75.4 ± 0.2
5	970	10.95	3.191	1.718	7.98	15.3	95.9	10.66	92.2 ± 0.2
6	990	11.5	3.231	1.934	9.83	22.4	95.7	11.15	96.4 ± 0.3
7	1000	12.4	3.208	2.265	9.86	29.5	95.2	11.95	103.2 ± 0.3
8	1010	13.15	3.197	2.223	8.14	35.4	95.2	12.72	109.5 ± 0.4
9	1020	14.24	3.201	2.471	7.35	40.8	95	13.73	118.0 ± 0.5
10	1040	28.27	3.233	2.176	9.82	47.9	97.6	27.87	231.9 ± 0.6
11	1060	34.56	3.355	1.339	21.8	63.7	98.5	34.44	282.5 ± 0.9
12	1070	23.72	3.508	1.784	12.9	73	97.9	23.45	197.1 ± 1.1
13	1080	16.42	3.128	8.699	2.14	74.6	81.2	14.07	120.8 ± 0.4
14	1090	14.25	3.283	10.02	2.67	76.5	76.8	11.51	99.4 ± 0.7
15	1120	17.66	3.36	1.082	26.8	95.9	97.3	17.58	149.7 ± 0.4
16	1140	24.82	3.482	21.69	1.26	96.8	69.6	18.66	158.6 ± 0.7
17	1200	23.77	3.6	12.1	3.86	99.6	82.6	20.45	173.1 ± 0.6
18	1450	21.58	3.456	8.246	0.555	100	6.6	19.39	164.5 ± 1.4
SINGLE CRYSTAL LASER FUSIONS (J=0.007323)									
1	>1450	9.945	2.899	1.148	3.69		98.2	9.788	124.9±0.8
2	"	5.32	3.128	1.759	2.73		93.5	4.992	64.8±1.2
3	"	19	2.922	1.704	2.46		98.2	18.69	231.4±1.6
4	"	2.388	3.392	1.814	2.18		85.5	2.057	27.0±1.9
5	"	2.396	3.094	2.322	2.3		78.5	1.895	24.9±1.5

APPENDIX 1B

Whole rock major element chemistry of samples analyzed.

ELEMENT	BULL-1	ELLN-4	ELLN-10	ELLN-7	PENL-14	PENL-13	PENL-12	PENL-3
SiO2	63.35	53.82	52.10	68.19	63.02	64.01	55.21	34.40
Al2O3	18.06	17.02	15.73	17.05	17.32	18.09	19.39	12.60
FeO	3.51	7.69	8.18	2.07	3.90	3.68	4.45	17.73
MgO	1.02	3.47	5.59	0.69	1.51	1.23	1.38	9.18
MnO	0.14	0.17	0.13	0.14	0.14	0.14	0.17	0.40
CaO	5.34	7.88	6.70	3.02	5.07	4.89	5.74	13.74
Na2O	5.01	3.97	3.49	5.60	5.03	5.29	6.50	4.34
K2O	1.90	1.86	1.41	2.77	2.01	2.23	4.37	1.61
TiO2	0.40	0.88	0.80	0.22	0.45	0.44	0.52	1.83
P2O5	0.14	0.30	0.25	0.08	0.15	0.20	0.21	1.88
LOI	0.41	1.83	4.75	0.26	0.70	1.90	0.81	0.67
TOTAL	99.27	98.89	99.11	100.09	99.30	102.10	98.75	98.38

ELEMENT	PENL-9	HILL-10KRS	ELL-1KRS	MW-2	MW-17	MW-13	TUK-1	TUK-2	TUK-6
SiO2	62.45	62.07	62.67	67.17	60.32	62.39	61.43	61.60	62.02
Al2O3	19.50	17.94	17.82	16.86	19.54	16.90	19.70	17.88	18.12
FeO	2.12	4.26	3.98	2.06	1.82	4.03	1.67	3.81	4.49
MgO	0.49	1.30	1.28	0.41	0.10	1.47	0.16	0.99	1.55
MnO	0.14	0.14	0.14	0.14	0.13	0.14	0.14	0.14	0.13
CaO	2.70	5.45	4.36	0.92	1.17	3.46	1.10	4.61	3.66
Na2O	6.63	5.16	5.89	7.26	9.33	7.52	9.07	7.36	4.52
K2O	4.70	1.99	2.23	5.56	5.46	3.42	5.33	2.48	3.43
TiO2	0.24	0.49	0.50	0.27	0.16	0.52	0.15	0.49	0.62
P2O5	0.06	0.18	0.19	0.08	0.03	0.24	0.02	0.19	0.21
LOI	1.15	1.01	1.33	0.29	1.09	0.59	1.60	1.31	1.45
TOTAL	100.18	99.99	100.39	101.02	99.15	100.68	100.37	100.86	100.20